Development 135, 2729-2738 (2008) doi:10.1242/dev.024539

Maternal depletion of CTCF reveals multiple functions during oocyte and preimplantation embryo development

Le-Ben Wan[1], Hua Pan[2], Sridhar Hannenhalli[3], Yong Cheng[4], Jun Ma[2], Andrew Fedoriw[1,*], Victor Lobanenkov[5], Keith E. Latham[4], Richard M. Schultz[2] and Marisa S. Bartolomei[1,†]

CTCF is a multifunctional nuclear factor involved in epigenetic regulation. Despite recent advances that include the systematic discovery of CTCF-binding sites throughout the mammalian genome, the in vivo roles of CTCF in adult tissues and during embryonic development are largely unknown. Using transgenic RNAi, we depleted maternal stores of CTCF from growing mouse oocytes, and identified hundreds of misregulated genes. Moreover, our analysis suggests that CTCF predominantly activates or derepresses transcription in oocytes. CTCF depletion causes meiotic defects in the egg, and mitotic defects in the embryo that are accompanied by defects in zygotic gene expression, and culminate in apoptosis. Maternal pronuclear transfer and CTCF mRNA microinjection experiments indicate that CTCF is a mammalian maternal effect gene, and that persistent transcriptional defects rather than persistent chromosomal defects perturb early embryonic development. This is the first study detailing a global and essential role for CTCF in mouse oocytes and preimplantation embryos.

KEY WORDS: CTCF, Mouse, Oocyte, Preimplantation embryo, Meiosis

INTRODUCTION

CTCF is an 11 zinc-finger DNA-binding protein that is highly conserved among species, and is expressed in almost all cell types (Filippova, 2008; Ohlsson et al., 2001). It was initially isolated as a factor that binds the *Myc* promoter and represses transcription (Lobanenkov et al., 1990). CTCF has since been shown to function as both a classical repressor and activator of transcription. Moreover, it carries out a multitude of other nuclear functions that depend on genomic and epigenetic context. For example, CTCF was identified as an enhancer blocker at the β-globin locus (Bell et al., 1999), and is the only known protein required for insulator activity in vertebrates. It can interact with both DNA and itself, providing a means by which CTCF molecules bound at remote sites in the genome can be brought together physically. According to a model for vertebrate insulator activity, this would prevent enhancer-promoter interactions between elements on different chromatin loops, while allowing or even facilitating those interactions within the same loop (Engel and Bartolomei, 2003; Wallace and Felsenfeld, 2007). Additionally, CTCF can tether its binding sites to the nucleolus, consistent with a model in which CTCF anchors chromatin loops to nuclear substructures (Yusufzai et al., 2004).

Subsequent to its discovery as an enhancer blocker at the β-globin locus, CTCF was shown to bind four elements within the imprinting control region (ICR) of the *H19/Igf2* locus (Bell and Felsenfeld, 2000; Hark et al., 2000; Kanduri et al., 2000; Szabo et al., 2000). CTCF binds to the maternal ICR, where it prevents the activation of *Igf2* by downstream enhancers that are shared by *H19* and *Igf2*. This allows *H19* exclusive access to enhancers on the maternal allele. On the paternal ICR, DNA methylation prevents CTCF from binding, allowing *Igf2* access to the shared enhancers. Thus, CTCF serves as a methylation-sensitive DNA-binding factor that mediates enhancer blocking at the imprinted *H19/Igf2* locus. Furthermore, CTCF binding is essential for preventing ectopic methylation on the maternal ICR (Engel et al., 2006; Pant et al., 2003; Szabo et al., 2004).

Additional CTCF-binding sites are described at other imprinted loci and on the X-chromosome, where they are proposed to play a regulatory role (Chao et al., 2002; Fitzpatrick et al., 2007; Hikichi et al., 2003; Yoon et al., 2005). Other CTCF-binding sites are located at boundaries between active and repressive chromatin, pointing to a role for CTCF at barrier elements (Barski et al., 2007; Cho et al., 2005; Filippova, 2008). Recently, thousands of CTCF-binding sites have been identified throughout the genome, consistent with a global role for CTCF in chromatin organization (Barski et al., 2007; Kim et al., 2007; Xie et al., 2007). Moreover, CTCF-binding sites overlap with cohesin-binding sites, and CTCF is essential for localizing cohesins to defined sites in the genome (Parelho et al., 2008; Stedman et al., 2008; Wendt et al., 2008). However, despite significant advances made in the past year, there are still no published data describing *Ctcf* deletions in mouse. Moreover, although CTCF has been depleted in mammalian cell culture using RNAi, the in vivo consequences of CTCF depletion are largely unknown. Thus, important physiological aspects of CTCF function remain undescribed, particularly the relevance of CTCF-binding sites throughout the genome, in different tissues of an adult organism and during development.

To understand the role of CTCF at the *H19/Igf2* locus, we previously generated transgenic mice expressing Ctcf dsRNA that depletes CTCF from growing oocytes (Fedoriw et al., 2004). The resulting oocytes are hypermethylated at the *H19* ICR. Moreover, the incidence of development to the blastocyst stage is markedly reduced. To gain insight into the molecular basis of these observations, we now identify hundreds of genes that are misregulated in CTCF-depleted oocytes using microarrays. More genes are downregulated than upregulated; moreover,

[1]Department of Cell and Developmental Biology, University of Pennsylvania School of Medicine, Philadelphia, PA 19104, USA. [2]Department of Biology, University of Pennsylvania, Philadelphia, PA 19104, USA. [3]Department of Genetics and Penn Center for Bioinformatics, University of Pennsylvania, Philadelphia, PA 19104, USA. [4]The Fels Institute for Cancer Research and Molecular Biology, and Department of Biochemistry, Temple University School of Medicine, Philadelphia, PA 19140, USA. [5]Laboratory of Immunopathology, NIAID, NIH, Rockville, MD 20852, USA.

*Present address: Department of Genetics, University of North Carolina, Chapel Hill, NC 27599, USA
†Author for correspondence (e-mail: bartolom@mail.med.upenn.edu)

Accepted 15 June 2008

downregulated genes are preferentially closer to CTCF-binding sites, especially in their upstream regions. These results are consistent with a major role for CTCF in transcriptional activation and derepression. In the oocyte, CTCF depletion delays the onset of meiosis and reduces meiotic competence, while preventing chiasmata resolution in a small proportion of eggs that have undergone polar body extrusion. After fertilization, CTCF-depletion delays the second mitotic division, perturbs zygotic genome activation, causes abnormal nuclear morphology and finally leads to apoptotic death prior to the blastocyst stage. Maternal pronuclear transfer and *Ctcf* mRNA microinjection experiments indicate that the two-cell delay is a maternal effect that is not caused by persistent chromatin changes arising in the egg, but is more likely to be caused by persistent transcriptional defects. Thus, *Ctcf* is a mammalian maternal effect gene that affects transcription during oocyte growth, and plays important independent roles in meiotic maturation and early embryonic development.

MATERIALS AND METHODS

Collection and culture of eggs and embryos

Transgenic (Tg) and non-transgenic (Ntg) female mice were genotyped as previously described (Fedoriw et al., 2004). Growing oocytes were collected from 10-day-old Tg and Ntg littermates. Fully-grown germinal vesicle (GV) oocytes were collected from 8- to 10-week-old littermates, and cultured in CZB medium at 37°C in an atmosphere of 5% CO_2 and air. Fertilized one-cell embryos were collected from superovulated and naturally plugged 8- to 10-week-old mice, and cultured in KSOM+AA medium (Ho et al., 1995) at 37°C in an atmosphere of 5% CO_2, 5% O_2 and 90% N_2. All experiments involving mice were approved by the University of Pennsylvania Institutional Animal Care and Use Committee.

Immunofluorescence and TUNEL staining

Cells were fixed with 2% paraformaldehyde for 25 minutes at room temperature. Embryos were TUNEL stained using In Situ Death Detection Kit (Roche). Immunofluorescence staining was done as previously described (Fedoriw et al., 2004). The antibody working dilutions were 1:3 (anti-CTCF, BD Biosciences, 612149), 1:100 (anti-H2AZ, Abcam, ab4174), 1:500 (anti-SMC1, Bethyl Labs, A300-055A) and 1:1000 (anti-dimethylH3K4, Upstate, 07030; anti-HP1-β, Chemicon, MAB3448; anti-α-Tubulin, Sigma, T6199). For SMC1 staining, embryos were pooled and extracted with 0.1% Triton X-100 prior to fixation. Images were acquired using confocal microscopy (Leica) and mean nuclear fluorescence was quantified using ImageJ v1.36b software.

Karyotyping eggs

Chromosome spreads were prepared as previously described (Tarkowski, 1966). Diakinesis spreads were prepared from eggs having undergone germinal vesicle breakdown (GVBD) by 2 hours post-culture. Metaphase II spreads were prepared from eggs having undergone PBE by 16 hours post-culture. Chromosome spreads were prepared from embryos arrested in prometaphase with 0.04 μg/μl colcemid for 1-2 or 16 hours.

RNA isolation and microarray analysis

GV oocytes were collected from 8- to 10-week-old superovulated mice. Five pairs of Ntg and Tg littermates from five different litters were used. Total RNA was extracted from pools of 25 oocytes per mouse using PicoPure RNA Isolation Kit (Acturus). cDNA was synthesized, amplified and biotin-labeled as previously described (Pan et al., 2005). One Affymetrix MOE430 2.0 GeneChip per mouse was probed with 15 μg cDNA and processed according to Affymetrix instructions. GeneChip tabular data are available at the Gene Expression Omnibus repository (www.ncbi.nlm.nih.gov/geo; accession #GSE11664). Raw microarray data were analyzed as previously described using MAS5, GeneSpring v7, SAM and EASE software (Pan et al., 2005). We used a 1.4-fold cutoff for EASE analysis because four biological replicates provided sufficient statistical power and confidence to detect a 1.4-fold change in transcript abundance (Zeng et al., 2004).

Real-time PCR

Total RNA was extracted from GV oocytes using Absolutely RNA Microprep Kit (Stratagene), and reverse transcribed using Superscript II reverse transcriptase (Invitrogen) and random hexamer primers. cDNA was quantified by real-time PCR using an ABI Prism 7000 thermocycler and Taqman probes (Applied Biosystems; Ctcf, Mm00484027_m1; Pim1, Mm00435712_m1; Cbfa2t1h, Mm00486771_m1; Gtl2, Mm00522599_m1; Grb10, Mm01180444_m1; Myc, Mm00487803_m1; Boris/Ctcfl, Mm01242223_m1; Slc22a18, Mm00485426_m1; Phlda2, Mm00493899_g1; Fcgr1, Mm00438874_m1; Tlr1, Mm00446095_m1; Ubft, Mm00456972_m1). Crossing points were normalized to UBTF and converted to relative expression values representing the average of three Tg samples over three Ntg samples. Each sample was analyzed in duplicate wells.

TRC upregulation

Fertilized one-cell embryos were collected from 8- to 10-week-old littermates 24 hours post-hCG, and cultured in CZB medium at 37°C in an atmosphere of 5% CO_2 and air. Embryos were examined for cleavage at 30-minute time intervals, and those that cleaved within a 2-hour time period were cultured for an additional 6, 12 and 21 hours. Embryos were then radiolabeled with 1 μCi/μl [^{35}S]-methionine/CZB, as previously described (Conover et al., 1991). Samples were separated using 10% SDS-PAGE and exposed to a phosphoimager. TRC levels were quantified using ImageQuant TL v2005 software.

Maternal pronuclear transfer experiments

One-cell embryos were collected from 8- to 10-week-old littermates 19 hours post-hCG. Maternal pronuclear transfer was carried out as described (Han et al., 2005). Embryos were cultured until 72 hours post-hCG in KSOM+AA medium at 37°C in an atmosphere of 5% CO_2, 5% O_2 and 90% N_2.

Production of Ctcf mRNA and microinjection

An optimized Kozak sequence was added upstream of the start codon at position 307 of a mouse CTCF cDNA sequence p5.1 (GB accession #U51037) subcloned into a Bluescript plasmid (Filippova et al., 1996). The CTCF-coding sequence, 66 bp of the modified 5′ UTR, and the first 267 bp of the 3′ UTR were then subcloned into an In-Vitro Transcription plasmid (pIVT) containing a synthetic poly(A) tail. Capped and polyadenylated *Ctcf* mRNA was transcribed using MEGAscript Kit (Ambion). RNA was purified using MEGAclear Kit (Ambion), precipitated and resuspended at 2 μg/μl in water. One-cell embryos were collected from 8- to 10-week-old littermates 19 hours post-hCG, and microinjected with 5-10 pl of Ctcf mRNA at a concentration of 1 or 2 μg/μl. Control embryos were injected with an equivalent amount of *Gfp* mRNA. Embryos were cultured until 72 hours post-hCG in KSOM+AA medium at 37°C in an atmosphere of 5% CO_2, 5% O_2 and 90% N_2.

Statistical analysis

Graphpad Prism 4 software was used to calculate statistical significance. Two-tailed *t*-tests, one-way ANOVA or Fisher's exact tests were used as appropriate.

RESULTS

CTCF depletion in oocytes and embryos

We previously generated Tg mice expressing Ctcf dsRNA under the control of the zona pellucida 3 (*Zp3*) promoter (Fedoriw et al., 2004). The transgene depletes CTCF specifically in growing oocytes because the *Zp3* promoter is active only in these cells. Five independent Tg lines have been previously described (Fedoriw et al., 2004). Depending on the line, Ctcf transcripts were reduced in fully-grown germinal vesicle (GV) oocytes by 50% to 99% relative to controls. We selected the three most severely affected lines for further study, all of which produced GV oocytes that were similarly CTCF-depleted (> 99% reduction; Table 1). Nevertheless, the three Tg lines exhibited phenotypic differences, described below, that

Table 1. Validation of gene misregulation by real-time PCR

Gene	Microarray Line 1	Real-time PCR Line 1	Line 12	Line 21
Ctcf	0.03	0.0094±0.0004	0.0094±0.003	0.0092±0.002
Pim1	0.48	0.62±0.06	0.54±0.26	0.38±0.06
Cbfa2t1h	0.55	0.61±0.06	0.62±0.15	0.69±0.08
Gtl2	0.55	0.53±0.08	0.51±0.02	0.55±0.05
Grb10	0.84	0.78±0.04	0.61±0.15	0.68±0.24
Myc	ND	1.05±0.12	0.91±0.35	0.86±0.18
Boris	ND	A:A	A:A	A:A
Slc22a18	1.77	2.80±0.18	1.88±0.50	1.94±0.21
Phlda2	1.86	2.18±0.23	1.55±0.15	2.16±1.15
Fcgr1	35.9	75.0±6.1	76.4±23.9	73.0±10.8
Tlr1	58.0	1:A	1:A	1:A

Values are transgenic expression relative to non-transgenic expression±s.e.m.
1:A, detected in transgenic oocytes but absent from non-transgenic oocytes.
A:A, absent from both transgenic and non-transgenic oocytes.
ND, not determined.

could have resulted from differences in the time course of CTCF depletion during oocyte growth. We therefore examined CTCF protein levels in growing oocytes, when the *Zp3* promoter controlling transgene expression is initially activated and maternal transcripts are beginning to accumulate. Growing oocytes from Line 1 were the most severely CTCF-depleted (86% reduction), followed by those from Line 21 (59% reduction) and Line 12 (33% reduction; Fig. 1A). CTCF mRNA levels correlated with protein levels (data not shown). Therefore, differences in CTCF depletion were apparent among the three most severely affected lines.

Although the *Zp3* promoter-driven transgene is only active during oocyte growth, RNAi probably persists in the GV oocyte, and for several cell divisions after fertilization (Wianny and Zernicka-Goetz, 2000). Persistent RNAi should affect all embryos derived from Tg females, regardless of whether the embryos themselves inherit the transgene. We therefore determined the protein expression patterns of CTCF in embryos derived from wild-type and Tg female littermates. In embryos derived from Ntg females, CTCF was excluded from nucleoli, but was otherwise diffusely localized in the nucleus throughout preimplantation development (Fig. 1B). CTCF was upregulated gradually from the morula to the late blastocyst stages of development (72 to 120 hours post-hCG). However, in embryos derived from Tg Line 1, CTCF was depleted through the morula and into the early blastocyst stages of development (72 and 96 hours post-hCG, respectively; Fig. 1B). Because zygotic CTCF is transcribed at the two-cell stage (48 hours post-hCG; data not shown), depletion of CTCF from later stages of preimplantation embryo development was most probably due to persistent RNAi (Fig. 1C).

Transcriptional misregulation in CTCF-depleted oocytes

Given the early and severe depletion of CTCF in Tg oocytes, and the multitude of CTCF-binding sites throughout the genome, we expected that many genes would be misregulated. We therefore compared the expression profiles of Tg and Ntg GV oocytes using Affymetrix MOE430 2.0 GeneChips, which cover over 39,000 transcripts and variants. Oocytes from five pairs of Ntg and Tg

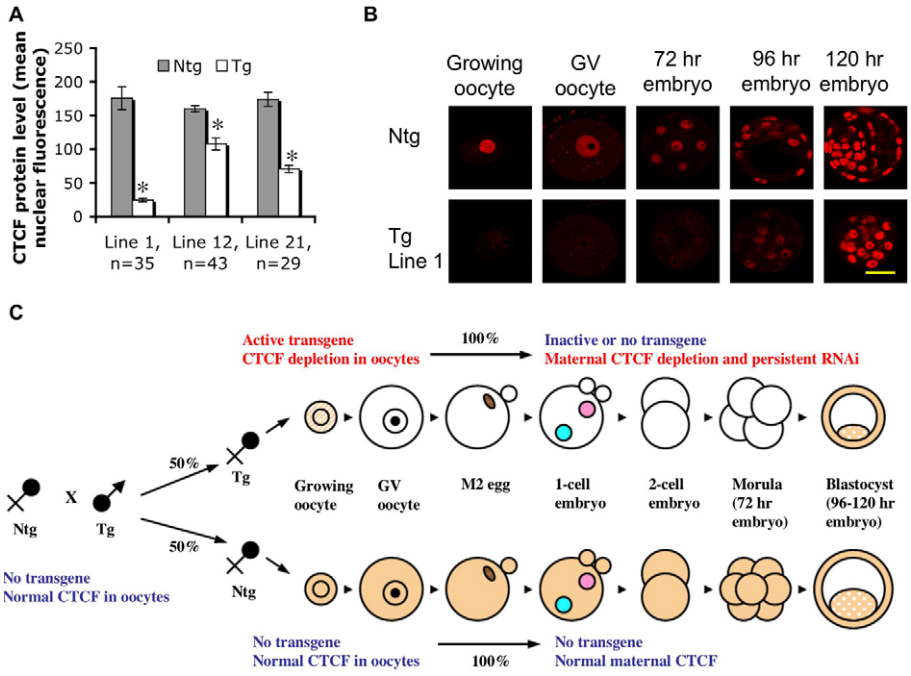

Fig. 1. CTCF depletion in oocytes and embryos. (**A**) Quantification of nuclear CTCF immunofluorescence staining in growing oocytes. Ntg and Tg indicate oocytes derived from 10-day-old Ntg and Tg littermates, respectively. Lines 1, 12 and 21 are shown. **P*<0.0001; *n*=number of oocytes. (**B**) Immunofluorescence images of CTCF-stained oocytes and embryos. One confocal section of an egg or embryo is shown per panel, with red indicating CTCF-stained nuclei. Line 1 is shown. Scale bar: 40 μm. (**C**) Schematic of CTCF depletion in oocytes and embryos. Ntg females were mated to Tg males and ~50% of female progeny inherited the transgene. All oocytes from Tg females were CTCF depleted. CTCF-replete oocytes and embryos are depicted in brown, whereas CTCF-depleted oocytes and embryos are depicted in white. Pink and blue circles represent maternal and paternal pronuclei, respectively. GV, germinal vesicle; hr, hours post-hCG.

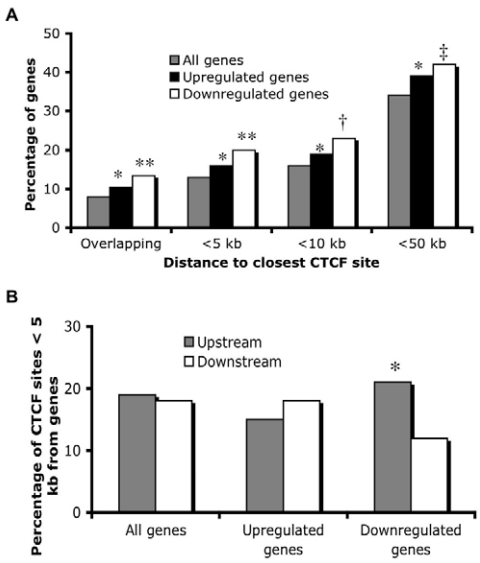

Fig. 2. Transcriptional misregulation in CTCF-depleted oocytes. (**A**) Percentages of genes within 0 (overlapping), 5, 10 and 50 kb of a CTCF-binding site. The proportions of nearby upregulated and especially downregulated genes were significantly higher than background (all genes) within every distance threshold. *P<0.05; **P<10^{-8}, $^{\dagger}P$<10^{-7}, $^{\ddagger}P$<10^{-5}. (**B**) Percentages of CTCF binding sites within 5 kb of all, upregulated and downregulated genes. Among sites within 5 kb of downregulated genes, the percentage of upstream sites was significantly higher than the percentage of downstream sites, compared with background. *P<0.05.

littermates were analyzed independently. To minimize false positives, we restricted analysis to 20,396 transcripts that were 'Present' according to Microarray Analysis Suite 5 (MAS5) software, in four out of five Ntg or Tg replicates. An unsupervised hierarchical cluster analysis revealed that all replicates clustered according to their genotype (see Fig. S1 in the supplementary material). Statistical Analysis of Microarrays (SAM) revealed 1590 significantly upregulated and 2282 significantly downregulated transcripts (FDR<5%). Of these transcripts, 460 were upregulated and 934 were downregulated by more than 1.4-fold, while 115 were upregulated and 278 were downregulated by more than twofold (see Table S1 in the supplementary material). Experimental Analysis Systematic Explorer (EASE) grouped 1.4-fold misregulated transcripts into several over-represented functional categories. (see Tables S2-S10 in the supplementary material). Interestingly, the most significantly over-represented categories were related to embryogenesis, suggesting that transcriptional defects in CTCF-depleted oocytes might affect subsequent embryonic development.

We then determined if CTCF-binding sites were enriched in areas of the genome near misregulated genes. We obtained the genomic locations of 5584 predicted and experimentally identified mouse CTCF sites from CTCFBSDB [(Bao et al., 2008); www.insulatordb.utmem.edu]. We obtained the genomic locations of all mouse genes from Ensemble Biomart (www.ensembl.org). For each mouse gene, we determined the distance to the closest CTCF-binding site, using 0 as the distance between a gene and an overlapping site. We found that upregulated and downregulated genes were both significantly closer to CTCF-binding sites than background, and this trend was strong up to a distance of 10 kb. In addition, the trend was much stronger for downregulated genes. For example, 13% of all genes, 16% of upregulated genes (P<0.05) and 20% of downregulated genes (P<10^{-8}) were located within 5 kb of a CTCF site (Fig. 2A). Next, we determined if CTCF binding sites were preferentially upstream or downstream of misregulated genes. Among CTCF sites within 5 kb of all genes, 19% were upstream and 18% were downstream of a gene. The remaining sites overlapped with genes. Among CTCF sites within 5 kb of upregulated genes, 15% were upstream and 18% were downstream. Most notably, among CTCF sites within 5 kb of downregulated genes, 21% were upstream and only 12% were downstream (P<0.05; Fig. 2B). Thus, among downregulated genes the closest CTCF-binding sites were significantly biased toward upstream locations. These results suggest that downregulated genes were CTCF targets rather than indirect targets or off-targets of RNAi. Moreover, considering that the majority of misregulated genes in CTCF-depleted oocytes was downregulated, these results suggest that CTCF predominantly activates or derepresses transcription in oocytes.

As expected, CTCF was the most highly downregulated gene (Table 1). We validated eight additional misregulated genes using real-time PCR (Table 1). Because several putative CTCF targets were not identified in our analysis, we examined two putative targets (*Myc* and *Ctcfl*/*Boris*) using real-time PCR. We found that although CTCF is a repressor of these genes in cell culture (Filippova et al., 1996; Qi et al., 2003; Vatolin et al., 2005), their expression was not upregulated in CTCF-depleted oocytes (Table 1). This is interesting in light of several studies showing that CTCF binding is largely invariant across cell lines (Gombert et al., 2003; Kim et al., 2007). It is therefore likely that the transcriptional output of CTCF binding varies in a cell-type specific manner, possibly as a consequence of different binding co-factors and post-translational modifications.

Meiotic defects in CTCF-depleted oocytes

Given the high level of transcriptional misregulation in CTCF-depleted oocytes, we examined oocyte nuclei using several anti-chromatin antibodies. Nuclear protein levels of dimethylH3K4, H2Az and HP1-β were unchanged in Tg oocytes derived from Line 1 (see Fig. S2A-F in the supplementary material). We also scored the numbers of surrounded nucleolus (SN)-type and non-surrounded nucleolus (NSN)-type GV oocytes, which can be distinguished based on nuclear morphology. NSN-type nuclei contain several discrete foci of heterochromatin on a background of decondensed euchromatin. Immediately prior to ovulation, NSN-type nuclei may transition to SN-type nuclei that are entirely heterochromatic and transcriptionally silent (Zuccotti et al., 1995). Although both subtypes can undergo meiotic maturation in vitro, SN-type oocytes are more meiotically competent (Liu and Aoki, 2002). Interestingly, we found that the frequency of the SN subtype was slightly but significantly decreased among Tg oocytes derived from all three lines (Table 2).

We therefore determined the rate of oocyte maturation by isolating and culturing GV oocytes, whereupon they resumed meiosis. At the end of prophase (diakinesis), the nuclear membrane dissolves and the apparent disappearance of the nucleus is known as germinal vesicle breakdown (GVBD). Slightly fewer Tg GV oocytes were able to undergo GVBD (data not shown). However, among oocytes that underwent GVBD, 26% of Ntg oocytes and only 2% of Tg oocytes had undergone GVBD by 1 hour post-culture. By 2 hours post-culture, roughly equal percentages of Ntg and Tg oocytes had undergone GVBD (Table 2). Thus, GVBD was delayed in CTCF-depleted oocytes. By 16 hours post-culture, 56% of Ntg oocytes and only 32% of Tg (Line 1) oocytes had extruded a polar body, signifying completion of meiosis I. A similar difference was

Table 2. Meiotic defects in CTCF-depleted oocytes

Line	Genotype	0 hours* % SN-type (*n*)	1 hour* % GVBD (*n*)	2 hours* % GVBD (*n*)	16 hours* % Ana/telo 1 (*n*)	16 hours* % PBE (n)
1	Ntg	68.7 (131)	26.0 (50)	76.0 (50)	9.5 (63)	55.6 (63)
	Tg	48.0 (98)	2.0 (50)	74.0 (50)	16.1 (62)	32.3 (62)
		P<0.01	*P*<0.001	*P*=1	*P*=0.3	*P*<0.05
12	Ntg	64.5 (110)	ND	ND	3.2 (62)	38.7 (62)
	Tg	57.6 (92)	ND	ND	6.2 (81)	24.7 (81)
		P=0.384			*P*=0.7	*P*=0.099
21	Ntg	81.5 (119)	ND	ND	4.8 (62)	58.1 (62)
	Tg	64.9 (111)	ND	ND	12.1 (66)	28.8 (66)
		P<0.01			*P*=0.21	*P*<0.01

*Germinal vesicle (GV) oocytes were cultured for the indicated number of hours.
SN-type, surrounded nucleolus-type GV oocytes.
GVBD, germinal vesicle breakdown.
Ana/telo 1, anaphase or telophase of meiosis 1.
PBE, polar body extrusion.
Ntg, non-transgenic; Tg, transgenic.
n, number of oocytes.
ND, not determined.

observed in all three Tg lines (Table 2). Longer periods of culture did not increase the incidence of polar body extrusion (PBE; data not shown). Thus, meiotic competence was decreased among CTCF-depleted oocytes.

To determine whether defects in chromosome segregation accompanied delayed meiotic maturation and decreased meiotic competence, we prepared diakinesis and metaphase-II chromosome spreads at 2 and 16 hours post-culture, respectively. By 2 hours post-culture, all Ntg and Tg eggs that underwent GVBD contained roughly 20 bivalents, and no obvious defects in chiasmata number or sister chromatid cohesion were apparent. By 16 hours post-culture, all Ntg eggs having undergone PBE contained roughly 20 univalents. However, although the majority of Tg eggs contained 20 apparently normal univalents, 7% of Tg eggs having undergone PBE contained roughly 20 bivalents (Fig. 3). Thus, PBE occurred in some Tg eggs without chiasmata resolution and chromosome segregation.

We observed no defects in spindle morphology using an antibody against α-tubulin (data not shown). However, we did find an increased proportion of Tg eggs in anaphase or telophase of metaphase 1, which presumably resulted from an overall delay in meiosis (Table 2). Eggs arrested at metaphase I can form 2n polar bodies upon fertilization, leading to digynic triploid embryos that die at various stages post-implantation (Kaufman and Speirs, 1987). Consistent with these observations, 8% of CTCF-depleted eggs formed triploid embryos when fertilized in vivo, whereas no Ntg eggs formed triploid embryos (see Fig. S3 in the supplementary material).

Early mitotic defects leading to apoptosis

We previously showed that although Tg eggs are fertilized in vitro at a normal incidence, fewer develop to the blastocyst stage by 120 hours post-hCG (Fedoriw et al., 2004). To determine when the decrease in developmental competence was first apparent, we cultured in vivo fertilized one-cell embryos and examined development at various time points after hCG injection. CTCF-depleted one-cell embryos cleaved at a normal rate, and by 48 hours post-hCG, almost all control and CTCF-depleted one-cell embryos reached the two-cell stage (data not shown). However, by 72 hours post-hCG, when control embryos were at the four- to eight-cell stage, CTCF-depleted embryos were at the two- to four-cell stage (Fig. 4A). Therefore, the decrease in developmental competence was first apparent at the two- to four-cell transition.

Because zygotic genome activation (ZGA) is essential for development beyond the two-cell stage, we determined whether ZGA was defective in CTCF-depleted embryos. An accepted marker for ZGA is the transcription requiring complex (TRC),

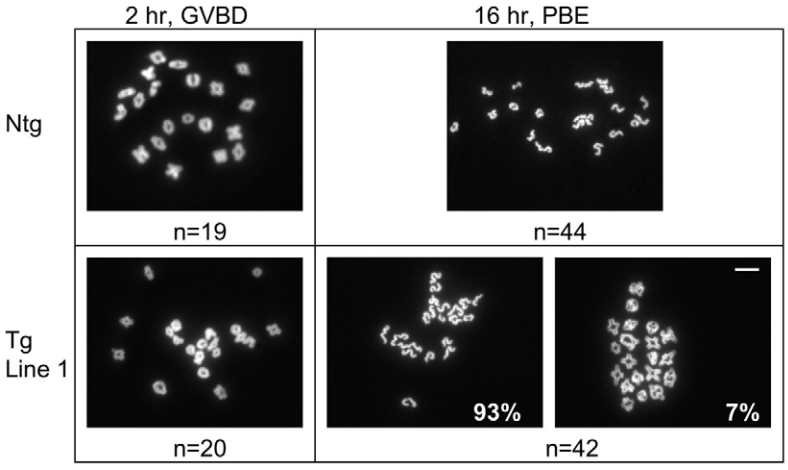

Fig. 3. Meiotic defects in CTCF-depleted oocytes. Eggs having undergone GVBD by 2 hours of culture were processed for diakinesis spreads. Eggs that have undergone PBE by 16 hours of culture were processed for M2 spreads. Line 1 is shown. Seven percent (3/42) of Tg eggs that have undergone PBE contained roughly 20 bivalents. *n*=number of oocytes. Scale bar: 0.1 μm.

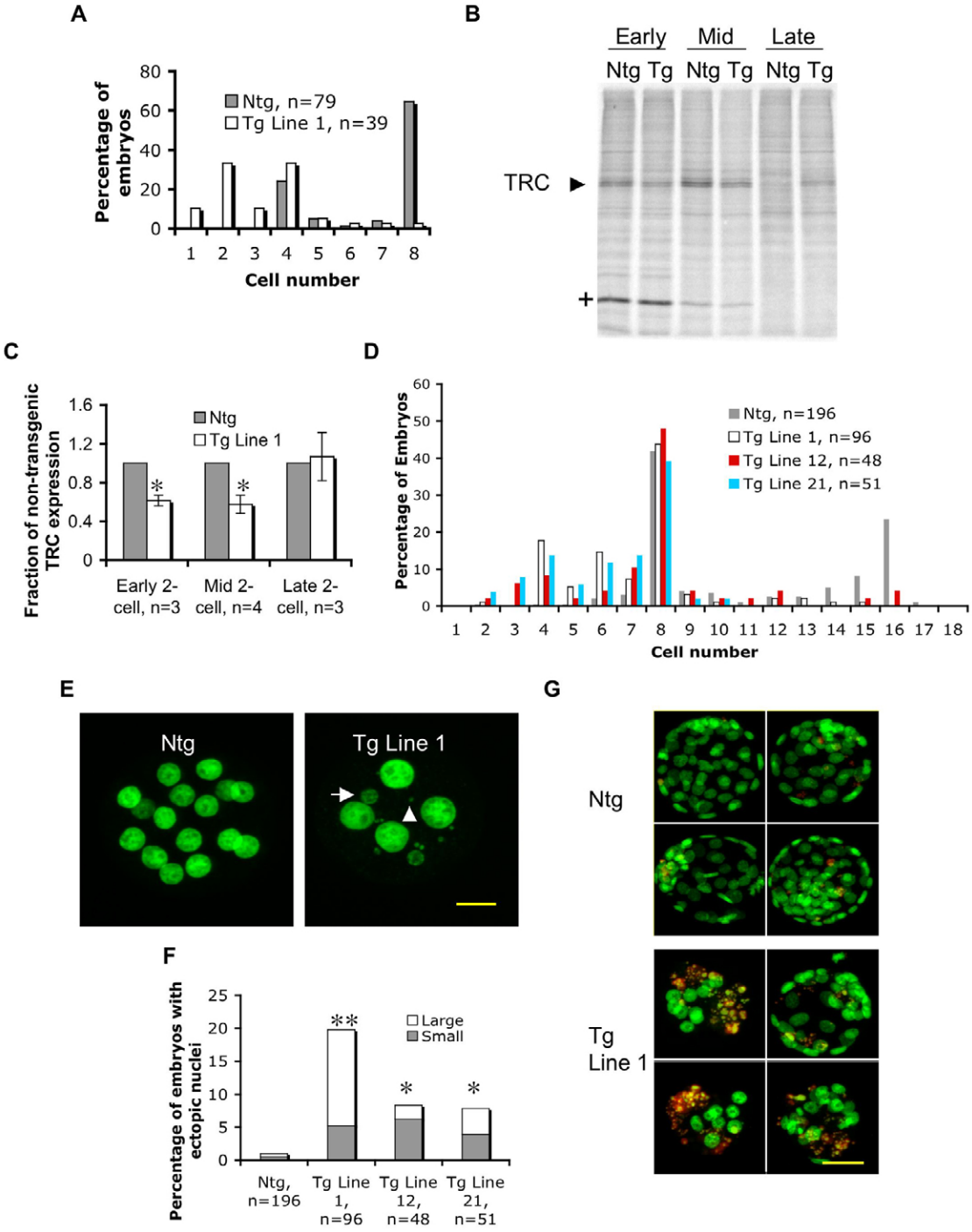

Fig. 4. Early mitotic defects leading to apoptosis. (**A**) Embryo development in culture. One-cell embryos were cultured to 72 hours post-hCG and categorized according to cell number. Line 1 is shown. *n*=number of embryos. (**B**) Autoradiogram and (**C**) quantification of TRC upregulation. Two-cell embryos from Line 1 were radiolabeled at various timepoints post-cleavage. At each timepoint, TRC expression in 3-5 embryos derived from Tg mice were normalized to TRC expression in an equivalent number of embryos derived from Ntg mice (relative expression=1). Early, Mid and Late indicate embryos radiolabeled at 6, 12 and 21 hours post-cleavage; **P*<0.05; *n*=number of experiments. + indicates Spindlin, an abundant maternal protein. (**D**) Embryo development in vivo. Cleavage-stage embryos were flushed at 72 hours post-hCG and categorized according to cell number. Lines 1, 12 and 21 are shown. *n*=number of embryos. (**E**) Immunofluorescence images of DAPI-stained embryos in D. One confocal section of an embryo is shown per panel, with green indicating DAPI-stained nuclei. Line 1 is shown. Tg embryos have ectopic nuclei. Arrow, large ectopic nucleus; arrowhead, small ectopic nucleus. Scale bar: 20 μm. (**F**) Percentages of embryos in D with ectopic nuclei. Embryos were categorized according to whether large (white bars) or small (gray bars) ectopic nuclei were observed. Lines 1, 12 and 21 are shown. **P*<0.05; ***P*<0.0001; *n*=number of embryos. (**G**) Apoptosis at 120 hours post-hCG. One-cell embryos were cultured to 120 hours post-hCG and TUNEL stained. One embryo is shown per panel, with green indicating DAPI-stained nuclei and red indicating TUNEL staining. Line 1 is shown. Only 7% (2/28) of embryos derived from Tg mice versus 94% (29/31) of embryos derived from Ntg littermates formed a blastoceol cavity by 120 hours post-hCG. Scale bar: 40 μm.

which is composed of three α-amanitin-sensitive proteins ~70 kDa in weight (Conover et al., 1991). In control two-cell embryos, TRC expression initiated by 6 hours after the first cleavage, peaked by 12 hours post-cleavage, and was downregulated by 22 hours post-cleavage. In CTCF-depleted two-cell embryos, TRC expression was reduced by 40% relative to control two-cell embryos at both 6 and 12 hours post-cleavage (Fig. 4B,C). It is therefore possible that a disruption in ZGA caused a developmental delay at the two-cell stage.

We also flushed cleavage-stage embryos from oviducts of Ntg and Tg females. By 72 hours post-hCG, embryos flushed from oviducts of Tg females were at the four- to eight-cell stage, whereas embryos flushed from oviducts of Ntg females were at the eight- to 16-cell stage (Fig. 4D). Thus, after spending more time at the two-cell stage, CTCF-depleted embryos were delayed by about one cell division, and this delay persisted at later timepoints (data not shown). Among cleavage-stage embryos flushed at 72 hours post-hCG, some exhibited abnormal ectopic nuclei (Fig. 4E). The frequency of embryos with ectopic nuclei was less than 1% among embryos derived from Ntg females, whereas the frequency was up to 20% among embryos derived from Tg females (Fig. 4F). Abnormal embryos were negative for cleaved caspase 3 and phosphorylated H2Ax (data not shown), indicating an absence of apoptosis or widespread DNA damage, but consistent with a mitotic defect leading to improper chromosome segregation.

In mammalian cell culture, CTCF is essential for localizing cohesins to specific sites throughout the genome; however, this localization is important for gene regulation at interphase rather than for sister chromatid cohesion during mitosis (Parelho et al., 2008; Stedman et al., 2008; Wendt et al., 2008). Consistent with these findings, mitotic chromosomes from CTCF-depleted two- to four-cell embryos exhibited no cohesion defects. Moreover, no significant differences in the rates of sister chromatid resolution or chromatid arm separation during mitotic arrest were observed, indicating that cohesins dissociated from chromatin normally during prophase and prometaphase (see Fig. S4A,B in the supplementary material). Finally, antibody staining of CTCF-depleted and control two- to four-cell embryos showed normal levels of chromatin-bound SMC1 during interphase (see Fig. S4C,D in the supplementary material).

By 120 hours post-hCG, 94% of cultured control embryos were at the blastocyst stage, whereas only 7% of cultured CTCF-depleted embryos were at the blastocyst stage. The remaining embryos were at the morula stage or at various stages prior to morula compaction. A limited amount of apoptosis is normal in blastocysts, and may be required to eliminate suboptimal blastomeres from the embryo prior to implantation. In agreement with previous reports (Fabian et al., 2005), we observed TUNEL-positive cells in the inner cell mass and trophectoderm of control blastocysts, but prior to 120 hours post-hCG only the polar body was TUNEL positive. Similarly, we did not observe apoptosis in CTCF-depleted embryos at earlier timepoints; however, by 120 hours post-hCG many CTCF-depleted embryos arrested at the morula stage exhibited abnormally high levels of apoptosis (Fig. 4G; data not shown). CTCF-depleted embryos having formed a blastoceol cavity appeared small but otherwise normal (Fig. 4G, upper left 'Tg' embryo). Thus, CTCF-depleted embryos failing to reach the blastocyst stage at the time of implantation were probably eliminated by apoptosis. Because CTCF levels were normal at this timepoint, apoptosis was presumably a downstream effect of earlier defects.

Maternal pronuclear transfer and Ctcf mRNA-injection experiments

Given the importance of CTCF in chromatin organization, we initially hypothesized that CTCF depletion caused a persistent nuclear change in the egg that resulted in the early mitotic defect. Such persistent changes could have included defects in meiosis or genome-wide epigenetic changes passed down from the egg and inherited by the embryo. To test this hypothesis, we performed maternal pronuclear transfer experiments in which maternal pronuclei of CTCF-depleted one-cell embryos were exchanged with maternal pronuclei of control one-cell embryos. By 48 hours after transfer, unmanipulated control embryos were at the four- to eight-cell stage, whereas unmanipulated CTCF-depleted embryos were at the two-cell stage. In control experiments, as expected, exchanging maternal pronuclei among control embryos or among CTCF-depleted embryos did not affect development. Surprisingly, introducing CTCF-depleted maternal pronuclei into control embryos resulted in development to the four- to eight-cell stage. These reconstructed embryos had normal nuclear CTCF protein levels by 48 hours after transfer, presumably because control embryos were replete with cytoplasmic stores of CTCF mRNA (Fig. 5A; data not shown). This result suggests that persistent nuclear changes arising in the egg did not cause the early mitotic defect, or that the changes could be reversed at the one-cell stage.

By contrast, introducing control maternal pronuclei into CTCF-depleted embryos resulted in development to the two-cell stage, suggesting that the early mitotic defect was caused by the depletion of maternal CTCF transcripts and possibly other maternal transcripts stored in the cytoplasm (Fig. 5A). However, persistent RNAi depleted CTCF until at least 48 hours after transfer, well after zygotic transcription of CTCF had begun (data not shown). Therefore, in order to separate maternal effects from the effects of persistent RNAi, we injected mouse *Ctcf* mRNA into one-cell embryos. By 48 hours after injection, control Gfp-injected embryos reached the four- to eight-cell stage, whereas CTCF-depleted Gfp-injected embryos reached the two- to four-cell stage. Injecting *Ctcf* mRNA into CTCF-depleted one-cell embryos restored nuclear protein levels by 6 and 48 hours after injection, but the resulting embryos were delayed at the two-cell stage (see Fig. S5 in the supplementary material; Fig. 5B,C). Therefore, maternal Ctcf transcripts were important for embryonic development, suggesting that CTCF is a maternal-effect gene. In addition, the data suggest that the two-cell delay was a consequence of transcriptional misregulation in the oocyte rather than a direct effect of CTCF depletion in the embryo.

DISCUSSION

Maternal-effect genes are transcribed in the oocyte, and are essential for normal embryonic development. To date, relatively few maternal effect genes have been identified in mammals. These include *Mater*, *Hsf1*, *Dnmt1o*, *Pms2*, *Stella*, *Npm2*, *Zar1*, *Formin2*, *mHR6a* and *E-cadherin*, all of which have been studied using traditional knockout technology (Burns et al., 2003; Christians et al., 2000; De Vries et al., 2004; Gurtu et al., 2002; Howell et al., 2001; Leader et al., 2002; Payer et al., 2003; Roest et al., 2004; Tong et al., 2000; Wu et al., 2003). However, useful this approach has been, it only uncovers maternal effect genes with relatively minor functions in other essential processes. Because ZGA in mammals occurs long before lineage specification and embryo patterning occur, many mammalian maternal effect genes could have important general functions that preclude the analysis of homozygous null females. More recent studies have used promoter-driven transgenes to deplete

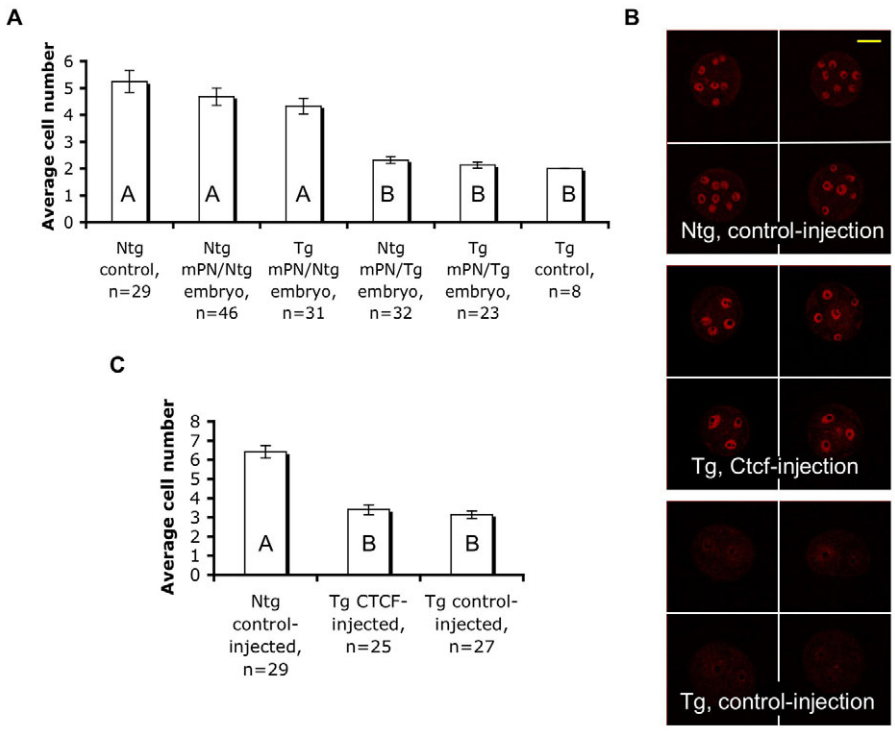

Fig. 5. Maternal pronuclear transfer and Ctcf mRNA-injection experiments. (**A**) Maternal pronuclear transfer experiments. Maternal pronuclei (mPNs) were reconstructed with one-cell embryos and cultured until 72 hours post-hCG. The average cell number per transfer-type at 72 hours post-hCG is indicated. Ntg and Tg (Line 1) indicate mPNs or embryos derived from Ntg and Tg littermates, respectively. Bars labeled A are significantly different from bars labeled B (overall $P<0.0001$). *n*=number of embryos. (**B**) Immunofluorescence images of CTCF-stained embryos after cytoplasmic mRNA microinjection. One-cell embryos from Line 1 were microinjected with CTCF or control GFP mRNA, and cultured until 72 hours post-hCG. One confocal section of an embryo is shown per panel, with red indicating CTCF-stained nuclei. Scale bar: 40 μm. (**C**) Embryo development after cytoplasmic mRNA microinjection. The average cell number per microinjection-type at 72 hours post-hCG is indicated. Bars labeled A are significantly different from bars labeled B (overall $P<0.0001$). *n*=number of embryos.

maternal transcripts without affecting maternal viability. For example, *Ezh2* and *Brg1* have been knocked out in growing oocytes using tissue-specific Cre/LoxP (Bultman et al., 2006; Erhardt et al., 2003), whereas basonuclin transcripts have been depleted from growing oocytes using transgenic RNAi (Ma et al., 2006).

Presently, there is no clear consensus on how directly a maternal gene influences embryonic processes in order for it to be considered a 'maternal-effect' gene. In many cases, maternal effects are believed to be independent of potential defects in oocyte growth and meiotic maturation, although this has only been proved in the case of *Brg1* (Bultman et al., 2006). However, in the case of *Formin2*, the maternal effect is clearly downstream of meiotic defects that lead to polyploidy and post-implantation lethality in the embryo (Leader et al., 2002). In many other cases, the molecular functions of maternal-effect genes and the full extent of their effects on oocyte development are simply unknown. Using transgenic RNAi, we have severely depleted CTCF from growing oocytes and identify hundreds of misregulated genes. However, despite such a high degree of gene misregulation in growing oocytes, the importance of CTCF does not become grossly apparent until meiotic maturation and the two-cell embryonic stage. In addition, we show that the two-cell mitotic defect is not the result of earlier meiotic defects or other persistent nuclear defects arising in the egg. Thus, *Ctcf* can be added to a short list of mammalian maternal effect genes, a list that will probably grow with the use of oocyte-specific gene-targeting methods.

Three recent studies have identified thousands of CTCF-binding sites throughout the human and mouse genomes (Barski et al., 2007; Kim et al., 2007; Xie et al., 2007). In the first study, a ChIP-Chip approach was used to identify 13,804 CTCF-binding sites, over 75% of which share a consensus motif (Kim et al., 2007). In the second study, a computational approach was used to identify 233 conserved noncoding elements (CNEs) (Xie et al., 2007). Three CNEs are bound by CTCF, and are found at 14,987 sites in the genome, which constitutes ~25% of the total number of sites identified. In the third study, a ChIP-Seq approach was used to identify 20,262 CTCF-binding sites (Barski et al., 2007). We have identified hundreds of misregulated genes in CTCF-depleted oocytes. The number of downregulated genes is greater than the number of upregulated genes, especially among highly misregulated genes. Moreover, downregulated genes are enriched for nearby CTCF-binding sites, especially in their upstream regions. Although it is likely that some transcriptional changes are indirect effects of CTCF depletion, the results suggest that many downregulated genes are direct CTCF targets. Moreover, the results are consistent with recent findings that CTCF-binding sites are enriched for active histone marks, and may activate genes by recruiting RNA polymerase II (Chernukhin et al., 2007) or by preventing the spread of heterochromatin. By contrast, upregulated genes are not as strongly associated with CTCF-binding sites, and nearby sites are not biased toward their upstream regions. These data could be consistent with CTCF acting as an enhancer-blocker to repress gene transcription from a distance, possibly by competing with promoters for nearby enhancers (Yoon et al., 2007) or by stalling the linear transfer of activating factors (Zhao and Dean, 2004). However, this mechanism of repression is less likely in oocytes and embryos prior to two-cell ZGA because, lacking a required co-factor, they apparently do not use enhancers (Majumder et al., 1997).

Given the multitude of CTCF-binding sites throughout the genome, and its diverse roles in nuclear organization, it is notable that in the absence of appreciable levels of CTCF, oocyte growth is apparently not perturbed, and defects in meiotic maturation are relatively minor. For example, only 7% of Tg oocytes fail to segregate chromosomes at anaphase I, and all oocytes can be fertilized regardless of meiotic defects. By contrast, after fertilization most CTCF-depleted embryos are delayed at the two-cell stage, and only 7% of CTCF-depleted embryos are able to form a blastoceol cavity. Moreover, maternal pronuclear transfer and RNA microinjection experiments suggest that persistent transcriptional defects rather than persistent chromatin defects result in the early

mitotic delay. Overall, these results point to an important role for CTCF in transcriptional regulation rather than in chromatin structure per se.

With respect to specific misregulated genes, several are imprinted. The maternally expressed transcript *Gtl2* is downregulated, consistent with a role for CTCF in transcriptional activation at the *Gtl2/Dlk1* locus (Paulsen et al., 2001). In addition, the maternally expressed gene *Grb10* is downregulated, and although CTCF is hypothesized to function as an insulator on the paternal allele (Hikichi et al., 2003), our results suggest that CTCF may activate *Grb10* on the maternal allele. However, two adjacent maternally expressed genes, *Slc22a18* and *Phlda2*, are upregulated. This is consistent with a role for CTCF in transcriptional repression at the *Kcnq1* locus (Fitzpatrick et al., 2007). Furthermore, the non-imprinted gene *Cbfa2t1h* is downregulated by almost twofold. *Cbfa2t1h* is a putative maternal effect gene that was identified as such because its transcripts are enriched in oocytes and one-cell embryos (Mager et al., 2006). However, *Cbfa2t1h* cannot easily account for the phenotypes because its protein levels appear only slightly decreased (data not shown). Nevertheless, it is possible that a combination of many transcriptional defects contribute to the phenotypes in CTCF-depleted embryos, or that a few highly misregulated genes have undiscovered maternal effects.

The two-cell delay and disruption of ZGA are consistent with a maternal effect because maternally derived products are presumed to regulate these early processes. We have yet to determine whether TRC expression in CTCF-depleted embryos is reduced throughout the two-cell stage, or if TRC expression peaks at a timepoint between 12 and 22 hours post-cleavage. In addition, we have not yet determined if other markers of ZGA are disrupted. However, with respect to TRC expression, there is a high degree of heterogeneity among small groups of CTCF-depleted two-cell embryos, and this heterogeneity increases as the two-cell stage progresses. This suggests that transcriptional defects in the oocyte may be compounded to varying degrees in individual embryos. Near the end of preimplantation development, a small number of embryos survive and implant. This may be a consequence of transcriptional heterogeneity during ZGA, or it may reflect differences in the time course of CTCF depletion among individual growing oocytes. This also implies that CTCF can restore chromatin organization and transcription de novo, but we do not know whether more subtle consequences of early CTCF-depletion persist. It will be interesting to determine what long-term epigenetic effects persist in CTCF-depleted embryos subsequent to implantation.

We thank Andrea Stout for help with confocal microscopy and statistical analysis, Paul Lieberman for providing cohesin antibodies, Patricia Hunt for providing chromosome spread protocols, and Joanne Thorvaldsen for helpful comments on the manuscript. This work was supported by NIH grant HD42026 to M.S.B. and R.M.S. L.B.W. was supported by US Public Health Service training grant GM08216. Y.C. and K.E.L. were supported by NIH/NCRR (RR018907). S.H. was supported by NIH GM078203.

Supplementary material

Supplementary material for this article is available at http://dev.biologists.org/cgi/content/full/135/16/2729/DC1

References

Bao, L., Zhou, M. and Cui, Y. (2008). CTCFBSDB: a CTCF-binding site database for characterization of vertebrate genomic insulators. *Nucleic Acids Res.* **36**, D83-D87.

Barski, A., Cuddapah, S., Cui, K., Roh, T. Y., Schones, D. E., Wang, Z., Wei, G., Chepelev, I. and Zhao, K. (2007). High-resolution profiling of histone methylations in the human genome. *Cell* **129**, 823-837.

Bell, A. C. and Felsenfeld, G. (2000). Methylation of a CTCF-dependent boundary controls imprinted expression of the *Igf2* gene. *Nature* **405**, 482-485.

Bell, A. C., West, A. G. and Felsenfeld, G. (1999). The protein CTCF is required for the enhancer blocking activity of vertebrate insulators. *Cell* **98**, 387-396.

Bultman, S. J., Gebuhr, T. C., Pan, H., Svoboda, P., Schultz, R. M. and Magnuson, T. (2006). Maternal BRG1 regulates zygotic genome activation in the mouse. *Genes Dev.* **20**, 1744-1754.

Burns, K. H., Viveiros, M. M., Ren, Y., Wang, P., DeMayo, F. J., Frail, D. E., Eppig, J. J. and Matzuk, M. M. (2003). Roles of NPM2 in chromatin and nucleolar organization in oocytes and embryos. *Science* **300**, 633-636.

Chao, W., Huynh, K. D., Spencer, R. J., Davidow, L. S. and Lee, J. T. (2002). CTCF, a candidate trans-acting factor for X-inactivation choice. *Science* **295**, 345-347.

Chernukhin, I., Shamsuddin, S., Kang, S. Y., Bergstrom, R., Kwon, Y. W., Yu, W., Whitehead, J., Mukhopadhyay, R., Docquier, F., Farrar, D. et al. (2007). CTCF interacts with and recruits the largest subunit of RNA polymerase II to CTCF target sites genome-wide. *Mol. Cell. Biol.* **27**, 1631-1648.

Cho, D. H., Thienes, C. P., Mahoney, S. E., Analau, E., Filippova, G. N. and Tapscott, S. J. (2005). Antisense transcription and heterochromatin at the DM1 CTG repeats are constrained by CTCF. *Mol. Cell* **20**, 483-489.

Christians, E., Davis, A. A., Thomas, S. D. and Benjamin, I. J. (2000). Maternal effect of Hsf1 on reproductive success. *Nature* **407**, 693-694.

Conover, J. C., Temeles, G. L., Zimmermann, J. W., Burke, B. and Schultz, R. M. (1991). Stage-specific expression of a family of proteins that are major products of zygotic gene activation in the mouse embryo. *Dev. Biol.* **144**, 392-404.

De Vries, W. N., Evsikov, A. V., Haac, B. E., Fancher, K. S., Holbrook, A. E., Kemler, R., Solter, D. and Knowles, B. B. (2004). Maternal beta-catenin and E-cadherin in mouse development. *Development* **131**, 4435-4445.

Engel, N. and Bartolomei, M. S. (2003). Mechanisms of insulator function in gene regulation and genomic imprinting. *Int. Rev. Cytol.* **232**, 89-127.

Engel, N., Thorvaldsen, J. L. and Bartolomei, M. S. (2006). CTCF binding sites promote transcription initiation and prevent DNA methylation on the maternal allele at the imprinted H19/Igf2 locus. *Hum. Mol. Genet.* **15**, 2945-2954.

Erhardt, S., Su, I. H., Schneider, R., Barton, S., Bannister, A. J., Perez-Burgos, L., Jenuwein, T., Kouzarides, T., Tarakhovsky, A. and Surani, M. A. (2003). Consequences of the depletion of zygotic and embryonic enhancer of zeste 2 during preimplantation mouse development. *Development* **130**, 4235-4248.

Fabian, D., Koppel, J. and Maddox-Hyttel, P. (2005). Apoptotic processes during mammalian preimplantation development. *Theriogenology* **64**, 221-231.

Fedoriw, A. M., Stein, P., Svoboda, P., Schultz, R. M. and Bartolomei, M. S. (2004). Transgenic RNAi reveals essentail function for CTCF in *H19* gene imprinting. *Science* **303**, 238-240.

Filippova, G. N. (2008). Genetics and epigenetics of the multifunctional protein CTCF. *Curr. Top. Dev. Biol.* **80**, 337-360.

Filippova, G. N., Fagerlie, S., Klenova, E. M., Myers, C., Dehner, Y., Goodwin, G., Neiman, P. E., Collins, S. J. and Lobanenkov, V. V. (1996). An exceptionally conserved transcriptional repressor, CTCF, employs different combinations of zinc fingers to bind diverged promoter sequences of avian and mammalian c-myc oncogenes. *Mol. Cell. Biol.* **16**, 2802-2813.

Fitzpatrick, G. V., Pugacheva, E. M., Shin, J. Y., Abdullaev, Z., Yang, Y., Khatod, K., Lobanenkov, V. V. and Higgins, M. J. (2007). Allele-Specific binding of CTCF to the multipartite Imprinting control region KvDMR1. *Mol. Cell. Biol.* **27**, 2636-2647.

Gombert, W. M., Farris, S. D., Rubio, E. D., Morey-Rosler, K. M., Schubach, W. H. and Krumm, A. (2003). The c-myc insulator element and matrix attachment regions define the c-myc chromosomal domain. *Mol. Cell. Biol.* **23**, 9338-9348.

Gurtu, V. E., Verma, S., Grossmann, A. H., Liskay, R. M., Skarnes, W. C. and Baker, S. M. (2002). Maternal effect for DNA mismatch repair in the mouse. *Genetics* **160**, 271-277.

Han, Z., Chung, Y. G., Gao, S. and Latham, K. E. (2005). Maternal factors controlling blastomere fragmentation in early mouse embryos. *Biol. Reprod.* **72**, 612-618.

Hark, A. T., Schoenherr, C. J., Katz, D. J., Ingram, R. S., Levorse, J. M. and Tilghman, S. M. (2000). CTCF mediates methylation-sensitive enhancer-blocking activity at the *H19/Igf2* locus. *Nature* **405**, 486-489.

Hikichi, T., Kohda, T., Kaneko-Ishino, T. and Ishino, F. (2003). Imprinting regulation of the murine Meg1/Grb10 and human GRB10 genes; roles of brain-specific promoters and mouse-specific CTCF-binding sites. *Nucleic Acids Res.* **31**, 1398-1406.

Ho, Y., Wigglesworth, K., Eppig, J. J. and Schultz, R. M. (1995). Preimplantation development of mouse embryos in KSOM: augmentation by amino acids and analysis of gene expression. *Mol. Reprod. Dev.* **41**, 232-238.

Howell, C. Y., Bestor, T. H., Ding, F., Latham, K. E., Mertineit, C., Trasler, J. M. and Chaillet, J. R. (2001). Genomic imprinting disrupted by a maternal effect mutation in the Dnmt1 gene. *Cell* **104**, 829-838.

Kanduri, C., Pant, V., Loukinov, D., Pugacheva, E., Qi, C. F., Wolffe, A., Ohlsson, R. and Lobanenkov, V. V. (2000). Functional association of CTCF with the insulator upstream of the H19 gene is parent of origin-specific and methylation-sensitive. *Curr. Biol.* **10**, 853-856.

Kaufman, M. H. and Speirs, S. (1987). The postimplantation development of spontaneous digynic triploid embryos in LT/Sv strain mice. *Development* **101**, 383-391.
Kim, T. H., Abdullaev, Z. K., Smith, A. D., Ching, K. A., Loukinov, D. I., Green, R. D., Zhang, M. Q., Lobanenkov, V. V. and Ren, B. (2007). Analysis of the vertebrate insulator protein CTCF-binding sites in the human genome. *Cell* **128**, 1231-1245.
Leader, B., Lim, H., Carabatsos, M. J., Harrington, A., Ecsedy, J., Pellman, D., Maas, R. and Leder, P. (2002). Formin-2, polyploidy, hypofertility and positioning of the meiotic spindle in mouse oocytes. *Nat. Cell Biol.* **4**, 921-928.
Liu, H. and Aoki, F. (2002). Transcriptional activity associated with meiotic competence in fully grown mouse GV oocytes. *Zygote* **10**, 327-332.
Lobanenkov, V. V., Nicolas, R. H., Adler, V. V., Paterson, H., Klenova, E. M., Polotskaja, A. V. and Goodwin, G. H. (1990). A novel sequence-specific DNA binding protein which interacts with three regularly spaced direct repeats of the CCCTC-motif in the 5′-flanking sequence of the chicken c-myc gene. *Oncogene* **5**, 1743-1753.
Ma, J., Zeng, F., Schultz, R. M. and Tseng, H. (2006). Basonuclin: a novel mammalian maternal-effect gene. *Development* **133**, 2053-2062.
Mager, J., Schultz, R. M., Brunk, B. P. and Bartolomei, M. S. (2006). Identification of candidate maternal-effect genes through comparison of multiple microarray data sets. *Mamm. Genome* **17**, 941-949.
Majumder, S., Zhao, Z., Kaneko, K. and DePamphilis, M. L. (1997). Developmental acquisition of enhancer function requires a unique coactivator activity. *EMBO J.* **16**, 1721-1231.
Ohlsson, R., Renkawitz, R. and Lobanenkov, V. (2001). CTCF is a uniquely versatile transcription regulator linked to epigenetics and disease. *Trends Genet.* **17**, 520-527.
Pan, H., O'Brien, M. J., Wigglesworth, K., Eppig, J. J. and Schultz, R. M. (2005). Transcript profiling during mouse oocyte development and the effect of gonadotropin priming and development in vitro. *Dev. Biol.* **286**, 493-506.
Pant, V., Mariano, P., Kanduri, C., Mattsson, A., Lobanenkov, V., Heuchel, R. and Ohlsson, R. (2003). The nucleotides responsible for the direct physical contact between the chromatin insulator protein CTCF and the H19 imprinting control region manifest parent of origin-specific long-distance insulation and methylation-free domains. *Genes Dev.* **17**, 586-590.
Parelho, V., Hadjur, S., Spivakov, M., Leleu, M., Sauer, S., Gregson, H. C., Jarmuz, A., Canzonetta, C., Webster, Z., Nesterova, T. et al. (2008). Cohesins functionally associate with CTCF on mammalian chromosome arms. *Cell* **132**, 422-433.
Paulsen, M., Takada, S., Youngson, N. A., Benchaib, M., Charlier, C., Segers, K., Georges, M. and Ferguson-Smith, A. C. (2001). Comparative sequence analysis of the imprinted Dlk1-Gtl2 locus in three mammalian species reveals highly conserved genomic elements and refines comparison with the Igf2-H19 region. *Genome Res.* **11**, 2085-2094.
Payer, B., Saitou, M., Barton, S. C., Thresher, R., Dixon, J. P., Zahn, D., Colledge, W. H., Carlton, M. B., Nakano, T. and Surani, M. A. (2003). Stella is a maternal effect gene required for normal early development in mice. *Curr. Biol.* **13**, 2110-2117.
Qi, C. F., Martensson, A., Mattioli, M., Dalla-Favera, R., Lobanenkov, V. V. and Morse, H. C., 3rd. (2003). CTCF functions as a critical regulator of cell-cycle arrest and death after ligation of the B cell receptor on immature B cells. *Proc. Natl. Acad. Sci. USA* **100**, 633-638.
Roest, H. P., Baarends, W. M., de Wit, J., van Klaveren, J. W., Wassenaar, E., Hoogerbrugge, J. W., van Cappellen, W. A., Hoeijmakers, J. H. and Grootegoed, J. A. (2004). The ubiquitin-conjugating DNA repair enzyme HR6A is a maternal factor essential for early embryonic development in mice. *Mol. Cell. Biol.* **24**, 5485-5495.
Stedman, W., Kang, H., Lin, S., Kissil, J. L., Bartolomei, M. S. and Lieberman, P. M. (2008). Cohesins localize with CTCF at the KSHV latency control region and at cellular c-myc and H19/Igf2 insulators. *EMBO J.* **27**, 654-666.
Szabo, P. E., Tang, S.-H., Rentsendorj, A., Pfeifer, G. P. and Mann, J. R. (2000). Maternal-specific footprints at putative CTCF sites in the *H19* imprinting control region give evidence for insulator function. *Curr. Biol.* **10**, 607-610.
Szabo, P. E., Pfeifer, G. P. and Mann, J. R. (2004). Parent-of-origin-specific binding of nuclear hormone receptor complexes in the H19-Igf2 imprinting control region. *Mol. Cell. Biol.* **24**, 4858-4868.
Tarkowski, A. K. (1966). An air-drying method for chromosome preparations for mouse eggs. *Cytogenetics* **5**, 394-400.
Tong, Z. B., Gold, L., Pfeifer, K. E., Dorward, H., Lee, E., Bondy, C. A., Dean, J. and Nelson, L. M. (2000). Mater, a maternal effect gene required for early embryonic development in mice. *Nat. Genet.* **26**, 267-268.
Vatolin, S., Abdullaev, Z., Pack, S. D., Flanagan, P. T., Custer, M., Loukinov, D. I., Pugacheva, E., Hong, J. A., Morse, H., 3rd, Schrump, D. S. et al. (2005). Conditional expression of the CTCF-paralogous transcriptional factor BORIS in normal cells results in demethylation and derepression of MAGE-A1 and reactivation of other cancer-testis genes. *Cancer Res.* **65**, 7751-7762.
Wallace, J. A. and Felsenfeld, G. (2007). We gather together: insulators and genome organization. *Curr. Opin. Genet. Dev.* **17**, 400-407.
Wendt, K. S., Yoshida, K., Itoh, T., Bando, M., Koch, B., Schirghuber, E., Tsutsumi, S., Nagae, G., Ishihara, K., Mishiro, T. et al. (2008). Cohesin mediates transcriptional insulation by CCCTC-binding factor. *Nature* **451**, 796-801.
Wianny, F. and Zernicka-Goetz, M. (2000). Specific interference with gene function by double-stranded RNA in early mouse development. *Nat. Cell Biol.* **2**, 70-75.
Wu, X., Viveiros, M. M., Eppig, J. J., Bai, Y., Fitzpatrick, S. L. and Matzuk, M. M. (2003). Zygote arrest 1 (Zar1) is a novel maternal-effect gene critical for the oocyte-to-embryo transition. *Nat. Genet.* **33**, 187-191.
Xie, X., Mikkelsen, T. S., Gnirke, A., Lindblad-Toh, K., Kellis, M. and Lander, E. S. (2007). Systematic discovery of regulatory motifs in conserved regions of the human genome, including thousands of CTCF insulator sites. *Proc. Natl. Acad. Sci. USA* **104**, 7145-7150.
Yoon, B., Herman, H., Hu, B., Park, Y. J., Lindroth, A., Bell, A., West, A. G., Chang, Y., Stablewski, A., Piel, J. C. et al. (2005). Rasgrf1 imprinting is regulated by a CTCF-dependent methylation-sensitive enhancer blocker. *Mol. Cell. Biol.* **25**, 11184-11190.
Yoon, Y. S., Jeong, S., Rong, Q., Park, K. Y., Chung, J. H. and Pfeifer, K. (2007). Analysis of the H19ICR Insulator. *Mol. Cell. Biol.* **27**, 3499-3510.
Yusufzai, T. M., Tagami, H., Nakatani, Y. and Felsenfeld, G. (2004). CTCF tethers an insulator to subnuclear sites, suggesting shared insulator mechanisms across species. *Mol. Cell* **13**, 291-298.
Zeng, F., Baldwin, D. A. and Schultz, R. M. (2004). Transcript profiling during preimplantation mouse development. *Dev. Biol.* **272**, 483-496.
Zhao, H. and Dean, A. (2004). An insulator blocks spreading of histone acetylation and interferes with RNA polymerase II transfer between an enhancer and gene. *Nucleic Acids Res.* **32**, 4903-4919.
Zuccotti, M., Piccinelli, A., Giorgi Rossi, P., Garagna, S. and Redi, C. A. (1995). Chromatin organization during mouse oocyte growth. *Mol. Reprod. Dev.* **41**, 479-485.

Table S1. Transcripts misregulated by more than twofold						
Gene symbol	UniGene	GenBank	Probeset ID*	Ntg raw value	Tg raw value	Tg/Ntg ratio
1110001J03Rik	Mm.158971	NM_025363	1416367_at	219	78	0.34
1110006O24Rik	Mm.133063	NM_021417	1420750_at	54	27	0.46
1110032A04Rik	Mm.45481	AF365876	1417802_at	44	21	0.42
1110032A04Rik	Mm.45481	AF365876	1417803_at	211	94	0.47
1110035H17Rik		AI450336	1453827_at	19	8	0.43
1110059M19Rik	Mm.336041	AV015858	1429135_at	77	36	0.49
1110065P19Rik; 2310040A07Rik		BB772205	1452893_s_at	11	36	**3.31**
1700021F05Rik	Mm.209953	BC013506	1421019_at	542	180	0.33
1700021F07Rik	Mm.46132	AK006200	1429803_at	296	903	**3.04**
1700023E05Rik	Mm.151092	AI848394	1447439_at	300	136	0.43
1700029I01Rik	Mm.276881	BQ033755	1436574_at	13	5	0.42
1700040D17Rik	Mm.87305	AV260432	1439559_at	41	18	0.37
1700086P04Rik		AK007024	1453479_at	69	30	0.44
1700113I22Rik	Mm.435537	AK007198	1432073_at	453	1096	**2.44**
1700129L04Rik	Mm.159041	NM_028588	1450328_at	12	5	0.33
1810012P15Rik	Mm.258932	AW108427	1436548_at	20	7	0.40
1810012P15Rik	Mm.258932	BM250236	1440234_at	18	9	0.47
1810020D17Rik	Mm.41583	BC026557	1451381_at	121	40	0.32
1810034K20Rik	Mm.24601	AK007694	1428337_at	22	8	0.35
1810034K20Rik	Mm.24601	NM_023397	1450067_a_at	22	3	0.08
1810046K07Rik	Mm.75315	AK007796	1453547_at	23	48	**2.09**
2200001I15Rik	Mm.27156	AA162958	1437019_at	122	56	0.45
2210013K02Rik	Mm.11112	AK008721	1431284_a_at	38	13	0.33
2210418O10Rik	Mm.229100	NM_029813	1449910_at	3	7	**2.25**
2310030B04Rik		BB144669	1438849_at	19	50	**2.57**
2310040A07Rik		BB772205	1428739_at	19	79	**4.11**
2310066E14Rik	Mm.41261	BC006820	1424239_at	114	54	0.48
2610002M06Rik	Mm.37274	NM_025921	1419690_at	50	14	0.26
2610005L07Rik; LOC546041	Mm.359054	BB471300	1437717_x_at	16	9	0.39
2810004I08Rik		BB825508	1453534_at	20	39	**2.08**
2810043G22Rik	Mm.242211	AK012899	1430934_at	88	32	0.36
3110057O12Rik	Mm.32373	AW061107	1429966_at	13	6	0.45
3222402P14Rik	Mm.335386	BF140684	1437869_at	7	14	**2.00**
4632404H12Rik	Mm.386816	BB216617	1438209_at	32	16	0.48
4632432E15Rik		AK014604	1432885_at	33	203	**5.72**
4733401H18Rik	Mm.29471	NM_023247	1418185_at	306	113	0.38
4921517B04Rik	Mm.379187	BB795572	1455377_at	18	9	0.48
4921517N04Rik	Mm.276415	AW488266	1429121_at	26	11	0.37
4930435F18Rik		AK015323	1431547_at	37	19	0.48
4930570C03Rik	Mm.28955	BC022913	1450409_a_at	93	29	0.32
4930570C03Rik	Mm.28955	BC022913	1450410_a_at	96	31	0.33
4930583I09Rik	Mm.109380	AK019827	1431669_at	44	14	0.33
4932443J21Rik		AV253967	1437272_at	9	4	0.34
4933404K13Rik		AK016653	1454567_at	13	7	0.45
4933426D04Rik		AK016926	1432407_at	18	36	**2.01**
5133401H06Rik		AK017223	1428663_at	10	3	0.36
5530401J07Rik		AK017436	1428796_at	14	7	0.49
5830443L24Rik	Mm.425261	NM_029509	1418776_at	15	8	0.48
6430550H21Rik	Mm.72979	BB520013	1436948_a_at	54	27	0.45
8030451N04Rik		BB400432	1455189_at	6	11	**2.02**
8430408J07Rik		AK018397	1453078_at	25	6	0.24
9530056K15Rik	Mm.188979	BB125017	1457523_at	23	8	0.29
9830115L13Rik		BB757349	1436183_at	44	17	0.36
9930012K11Rik	Mm.12148	AV223039	1433801_at	144	297	**2.05**
A130022J15Rik	Mm.251789	BI149851	1433671_at	33	9	0.29
A130022J15Rik	Mm.251789	BI149851	1454678_s_at	74	17	0.25

A330033J07Rik		BG067329	1458799_at	14	8	0.47
A330102K23Rik	Mm.102025	BG065199	1455516_at	64	33	0.48
A830058L05Rik	Mm.33443	BB271764	1457566_at	34	7	0.19
Abca9	Mm.291459	AW046072	1440879_at	74	31	0.42
Ablim3	Mm.329478	BM900139	1434013_at	119	34	0.29
Adprhl2	Mm.11285	BC023177	1427449_a_at	40	20	0.50
AI452195		BB303582	1435280_at	22	10	0.43
AI481121		BB498095	1456123_at	59	29	0.49
Akr1b8	Mm.5378	NM_008012	1448894_at	645	106	0.17
Alk	Mm.311854	NM_007439	1449987_at	99	36	0.38
Aof2	Mm.28540	AK007763	1426761_at	108	50	0.45
Aof2	Mm.28540	AK007763	1426762_s_at	474	202	0.43
Apba2	Mm.4657	BE952331	1427288_at	43	3	0.08
Arl2	Mm.21071	NM_019722	1422549_at	698	310	0.44
Art1	Mm.261071	U31510	1451372_a_at	32	12	0.37
Asb12	Mm.79122	NM_080858	1420346_at	67	23	0.34
Atn1	Mm.333380	NM_007881	1421149_a_at	26	64	**2.41**
Atp4a	Mm.12821	NM_018731	1421286_a_at	18	38	**2.13**
AU018091	Mm.268551	AV099404	1435154_at	204	90	0.45
AU019176		BM228311	1456179_at	52	20	0.39
AW049604	Mm.244319	BB804965	1419490_at	31	10	0.26
AW551984	Mm.208855	AV220682	1433434_at	33	17	0.47
B230112P13Rik		BQ175636	1439633_at	94	41	0.43
B230120H23Rik	Mm.314618	BB454974	1435029_at	59	19	0.29
B230396O12Rik	Mm.72944	AV274423	1446123_at	370	927	**2.45**
B3gnt1	Mm.29628	AV032053	1452346_at	137	64	0.48
Bai1	Mm.43133	BG261923	1455363_at	36	14	0.39
Basp1	Mm.29586	AK011545	1428572_at	109	222	**2.05**
BB182387		AV269187	1438885_at	2	9	**5.89**
BC013672	Mm.275233	BC013672	1451777_at	44	19	0.46
BC037703	Mm.32900	AV231983	1455241_at	64	15	0.24
BC067068	Mm.250875	BB811762	1434749_at	84	166	**2.02**
Bgn	Mm.2608	BC019502	1448323_a_at	39	20	0.49
Bmp7	Mm.595	NM_007557	1418910_at	11	33	**2.82**
Bsn	Mm.437679	BQ176524	1436123_at	9	32	**3.73**
Bsn	Mm.437679	AV139249	1450467_at	21	51	**2.50**
C030044B11Rik		AK021143	1429264_at	84	43	0.48
C1qbp	Mm.30049	AV108824	1455821_x_at	2027	906	0.44
C330008K14Rik	Mm.30649	BE985366	1436194_at	56	28	0.48
Cacnb2	Mm.313930	BG069383	1444693_at	17	7	0.39
Cacnb2	Mm.313930	W41214	1452476_at	32	15	0.48
Cacnb2	Mm.313930	BB078175	1456401_at	173	78	0.45
Capn1	Mm.6221	AF084459	1417228_at	41	18	0.45
Ccdc5	Mm.39293	BC024400	1424955_at	408	202	0.48
Ccl2	Mm.290320	AF065933	1420380_at	13	63	**5.18**
Cd163	Mm.37426	NM_053094	1419144_at	8	3	0.19
Cd1d1	Mm.1894	NM_007639	1449130_at	123	45	0.36
Cd200	Mm.245851	AF004023	1448788_at	205	107	0.50
Cd200r3	Mm.297337	BB749845	1453813_at	10	22	**2.06**
Cd24a	Mm.29742	NM_009846	1448182_a_at	2	8	**4.14**
Chrdl1	Mm.157697	AV144145	1434201_at	19	6	0.32
Clic3	Mm.44194	AK009020	1429574_at	16	37	**2.53**
Clps	Mm.21160	AV076302	1438612_a_at	12	2	0.23
Cnga1	Mm.436652	U19717	1451763_at	46	21	0.44
Crip2	Mm.133825	NM_024223	1417311_at	134	61	0.46
Ctcf	Mm.269474	BB836888	1418330_at	766	21	0.03
Ctcf	Mm.269474	BB836888	1449042_at	1001	36	0.04
Cttnbp2	Mm.224189	BB357580	1435435_at	63	28	0.48
Cubn	Mm.313915	AF197159	1426990_at	11	5	0.40
Cubn	Mm.313915	AF197159	1452270_s_at	27	13	0.49

Cxcl14	Mm.30211	AF252873	1418457_at	29	72	**2.42**
Cxcr4	Mm.1401	D87747	1448710_at	7	48	**6.24**
Cyb561d1	Mm.246391	BB016212	1459837_at	18	9	0.46
Cyp51	Mm.140158	NM_020010	1422533_at	8	16	**2.02**
D430042O09Rik	Mm.274389	BB487579	1443334_at	46	99	**2.19**
Dach2	Mm.79760	NM_033605	1449823_at	37	13	0.33
Dbil5	Mm.347413	AK006528	1421865_at	5	21	**3.99**
Dbt	Mm.3636	NM_010022	1449118_at	55	22	0.39
Dclk3	Mm.26361	BB326709	1436532_at	162	57	0.38
Ddit4l	Mm.250841	AF335325	1451751_at	3	11	**3.19**
Dennd4b	Mm.30571	BC026996	1427014_at	50	17	0.34
Dnajc5g	Mm.189696	BB667162	1437814_at	59	24	0.42
Dscr6	Mm.42604	NM_133229	1420459_at	8	16	**2.09**
Dtd1	Mm.28109	AI451865	1451040_at	77	506	**6.56**
Dtx3l	Mm.390852	AV327407	1435208_at	100	51	0.48
Dtx3l	Mm.390852	BB705351	1439825_at	37	18	0.44
Dync1i1	Mm.20893	NM_010063	1416361_a_at	92	44	0.47
E130311K13Rik	Mm.39342	BB754259	1439531_at	149	51	0.36
E430004N04Rik	Mm.123021	BB201286	1439719_at	38	20	0.49
Efhd1	Mm.247951	BC019531	1448507_at	55	198	**3.64**
Egflam	Mm.203208	AV024806	1434647_at	41	120	**2.99**
Enc1	Mm.241073	BM120053	1420965_a_at	30	12	0.38
Epha6	Mm.353171	NM_007938	1421527_at	10	21	**2.08**
Epha7	Mm.257266	BC026153	1451991_at	11	3	0.19
Eras	Mm.250895	AV212609	1456511_x_at	137	64	0.46
Etl4	Mm.237935	BM250266	1426880_at	179	470	**2.61**
F13b	Mm.30105	NM_031164	1419131_at	19	6	0.31
Fcgr1	Mm.150	AF143181	1417876_at	7	245	**35.89**
Fezf1	Mm.55115	AK014242	1429991_at	12	3	0.34
Flot1	Mm.2931	NM_008027	1448559_at	393	1663	**4.27**
Foxp2	Mm.432481	AV322952	1438231_at	98	36	0.39
Foxp2	Mm.432481	AV322952	1438232_at	55	23	0.41
Foxp2	Mm.432481	BM964154	1440108_at	58	18	0.32
Frmpd1	Mm.24783	BM213356	1435189_at	143	291	**2.00**
Fshr	Mm.57155	NM_013523	1450810_at	23	48	**2.05**
Fstl5	Mm.379337	BB374771	1439904_at	20	8	0.41
Ftl2; Ftl1	Mm.431913; Mm.30357	NM_008049	1422302_s_at	237	462	**2.08**
Fxn	Mm.7319	AV007132	1427282_a_at	40	15	0.34
Gca	Mm.219877	BC021450	1451451_at	7	13	**2.09**
Gcc1	Mm.332950	AV339946	1429033_at	36	83	**2.29**
Gimap8	Mm.86514	BM243674	1456061_at	41	15	0.38
Gja7	Mm.390369	AV148957	1447787_x_at	7	19	**2.29**
Gldc	Mm.274852	NM_138595	1416049_at	15	200	**13.43**
Gli3	Mm.5098	BB311687	1455154_at	189	417	**2.29**
Gli3	Mm.5098	AW546010	1456067_at	140	287	**2.09**
Gm1060	Mm.256588	BG070552	1455279_at	31	69	**2.28**
Gm1960	Mm.244289	BB829808	1438148_at	5	2	0.24
Gm566	Mm.297245	BG243248	1452614_at	44	16	0.35
Gm691	Mm.441156	BQ174072	1455714_at	90	44	0.46
Gpr125	Mm.272974	BG277370	1431034_at	33	18	0.48
Gpr177	Mm.6766	BC018381	1423824_at	16	8	0.49
Gpr62	Mm.326268	BE955672	1442138_at	4	8	**2.02**
H2-Aa	Mm.235338	BE688749	1435290_x_at	100	37	0.37
H2-Aa	Mm.235338	AV018723	1438858_x_at	29	12	0.38
Has3	Mm.56986	NM_008217	1420589_at	145	20	0.15
Hck	Mm.715	NM_010407	1449455_at	57	143	**2.51**
Hdgfrp3	Mm.221412	BB291880	1450924_at	9	23	**2.45**
Hes1	Mm.390859	BC018375	1418102_at	7	36	**5.14**

Hist1h3f; Hist2h3c; Hist1h3b; Hist1h3d; Hist1h3e; Hist1h3h; Hist1h3i; Hist2h3b	Mm.221389; Mm.383293; Mm.342457; Mm.347699; Mm.261658; Mm.377874; Mm.390558; Mm.358797	AK010121	1431231_at	87	40	0.46
Hmgn3	Mm.244426	AK002970	1431777_a_at	32	253	**8.43**
Hmgn3	Mm.244426	AV018952	1434875_a_at	105	1044	**10.36**
Hoxd1	Mm.4932	NM_010467	1420573_at	6	14	**2.33**
Hoxd8	Mm.280673	AA265122	1431099_at	26	72	**2.83**
Hs1bp3	Mm.309954	AW541327	1433843_at	38	10	0.28
Hspa1a	Mm.6388	AW763765	1452388_at	188	365	**2.09**
Htr5b	Mm.4833	NM_010483	1422196_at	12	29	**2.28**
Ick	Mm.288719	NM_019987	1448310_at	219	100	0.46
Idh1	Mm.9925	NM_010497	1422433_s_at	469	202	0.37
Igsf11	Mm.245564	BM899311	1460607_at	73	18	0.24
Igsf21	Mm.298731	BB769866	1433950_at	15	34	**2.25**
Il28ra	Mm.259623	AW212870	1460598_at	33	74	**2.39**
Inpp5e	Mm.330070	BM217803	1423229_at	74	35	0.48
Inpp5e	Mm.330070	BM217803	1423230_at	19	9	0.46
Irx1	Mm.316056	AF165984	1451983_at	15	37	**2.59**
Isx	Mm.158735	AK018615	1431922_at	14	32	**2.18**
Itgae	Mm.96	AV210813	1447541_s_at	49	210	**4.45**
Itgae	Mm.96	NM_008399	1449216_at	22	53	**2.32**
Kalrn		BB662566	1448023_at	380	102	0.25
Kalrn		BB560050	1457690_at	88	31	0.35
Kcna5	Mm.222831	NM_008419	1417680_at	7	15	**2.17**
Krt25	Mm.268173	NM_133730	1418173_at	95	40	0.46
Krt35	Mm.37952	NM_016880	1420409_at	12	28	**2.42**
Krt72	Mm.298210	AA791107	1419840_at	101	47	0.48
Krtcap2	Mm.177991	NM_025327	1417058_a_at	221	105	0.47
Krtcap2	Mm.177991	NM_025327	1417059_at	270	128	0.47
L3mbtl3	Mm.338439	BB022070	1434246_at	63	23	0.37
L3mbtl3	Mm.338439	BB022070	1454882_at	148	38	0.24
Lect2	Mm.16973	NM_010702	1449492_a_at	43	6	0.12
Lonrf2	Mm.296437	AK013739	1429965_at	53	110	**2.06**
Lrrtm3	Mm.244348	BB132359	1440112_at	105	39	0.36
Mak	Mm.8149	BG069426	1422725_at	10	22	**2.17**
Map2k6	Mm.14487	BB261602	1426850_a_at	94	43	0.48
Mapt	Mm.1287	M18775	1424719_a_at	6	27	**4.21**
Mar4	Mm.337023	BB260801	1441223_at	33	11	0.35
Mfhas1	Mm.103246	BB107412	1429005_at	141	46	0.33
Mfhas1	Mm.103246	BE225764	1436897_at	38	19	0.47
MGI:2660854	Mm.66952	AV271256	1439613_at	24	13	0.48
Minpp1	Mm.255116	AK017558	1429750_at	10	4	0.32
Morc1	Mm.250060	NM_010816	1419418_a_at	242	119	0.48
Mrpl23	Mm.12144	NM_011288	1416948_at	295	93	0.30
Mrps16	Mm.23747	NM_025440	1448869_a_at	555	1212	**2.20**
Mrps2	Mm.294951	AV031454	1420845_at	31	13	0.41
Mrps2	Mm.294951	AV031454	1420846_at	527	205	0.38
Mtmr6	Mm.247007	BC020019	1425485_at	31	11	0.36
Mtmr6	Mm.247007	BC020019	1425486_s_at	146	53	0.35
Mtmr6	Mm.247007	BB297632	1456540_s_at	92	32	0.33
Muc15	Mm.32566	BC020027	1426941_at	20	6	0.36
Mup2; Mup1	Mm.237772; Mm.335875	NM_031188	1420465_s_at	24	10	0.47
Myh11	Mm.250705	BC026142	1448962_at	354	179	0.50
Myl2	Mm.1529	NM_010861	1448394_at	21	44	**2.19**

Mylip	Mm.212855	BC010206	1424988_at	152	46	0.30
Ndufb7	Mm.29683	NM_025843	1416417_a_at	2243	926	0.41
Ndufb7	Mm.29683	NM_025843	1448331_at	456	212	0.48
Neu1	Mm.8856	AI649303	1416831_at	21	9	0.38
Npal3	Mm.26548	AK018640	1429241_at	53	25	0.44
Nr2c1	Mm.107483	NM_011629	1418605_at	200	49	0.24
Nr4a2	Mm.3507	BB703394	1455034_at	15	31	**2.00**
Nrp2	Mm.266341	BB752129	1435349_at	6	24	**4.10**
Nsbp1	Mm.298443	NM_016710	1418152_at	210	104	0.48
Nsmce4a	Mm.21714	AK010349	1428213_at	1175	399	0.34
Nsmce4a	Mm.21714	AV151371	1439461_x_at	72	36	0.49
Ntn1	Mm.39095	BI143915	1454974_at	43	20	0.45
Obfc2b	Mm.46614	BC026942	1451291_at	232	483	**2.09**
Ocrl	Mm.210343	BB751120	1438396_at	86	41	0.45
Olfm4	Mm.26456	AV290148	1437060_at	16	6	0.36
Osbpl7	Mm.379194	BB768954	1428893_at	115	62	0.50
Oxr1	Mm.254267	AW548944	1418501_a_at	24	86	**3.51**
Pcdh19	Mm.39738	BB053591	1437360_at	15	36	**2.40**
Pcdh19	Mm.39738	BB732600	1444422_at	9	23	**2.31**
Pcdhb15	Mm.283857	BB174795	1443421_s_at	19	4	0.17
Pcdhb17	Mm.87553	NM_053142	1448933_at	15	5	0.34
Pdha2	Mm.4223	AV206348	1450962_at	15	41	**2.75**
Pdzrn3	Mm.321654	NM_018884	1416846_a_at	334	779	**2.27**
Phlpp	Mm.24115	BC024670	1426994_at	57	22	0.37
Phyh	Mm.391704	NM_010726	1460194_at	84	213	**2.57**
Pigc	Mm.45106	AK014096	1424189_at	729	169	0.23
Pim1	Mm.328931	AI323550	1435458_at	260	126	0.48
Pink1	Mm.18539	AV371921	1441937_s_at	39	19	0.46
Plcb4	Mm.38009	BM730668	1435771_at	69	32	0.45
Plek	Mm.98232	AF181829	1417523_at	22	7	0.36
Plek	Mm.98232	AF181829	1448748_at	135	52	0.39
Plek	Mm.98232	AF181829	1448749_at	21	7	0.37
Plxna2	Mm.2251	BB085537	1429772_at	148	24	0.15
Plxna2	Mm.2251	D86949	1451753_at	186	54	0.29
Plxna2	Mm.2251	BB085537	1453286_at	238	59	0.25
Plxna2	Mm.2251	BB002869	1455037_at	152	45	0.29
Plxnb3		AI451018	1440813_s_at	27	12	0.43
Ppa2	Mm.210305	BC011417	1424488_a_at	262	92	0.34
Ppm1e	Mm.341988	BB346082	1434990_at	24	3	0.10
Prkg2	Mm.263002	BB823350	1435162_at	55	24	0.42
Prmt6	Mm.36115	BB233495	1457071_x_at	7	4	0.36
Ptgs2	Mm.292547	M94967	1417262_at	4	15	**3.30**
Ptprk	Mm.332303	AI893646	1423278_at	23	11	0.42
Pxdn	Mm.251774	AK010185	1428259_at	17	8	0.40
Pygl	Mm.256926	NM_133198	1417741_at	77	326	**4.31**
Rab24	Mm.220923	NM_009000	1421872_at	20	41	**2.05**
Rab32	Mm.31486	NM_026405	1416527_at	378	159	0.41
Raet1a; Raet1b; Raet1c; Raet1d; Raet1e	Mm.439724; Mm.440891	NM_009016	1420603_s_at	160	72	0.46
Rag1ap1	Mm.17958	NM_009057	1448948_at	25	10	0.40
Rarb	Mm.259318	BB266455	1454906_at	18	7	0.37
Rbm35b	Mm.183003	BF124648	1433683_at	15	33	**2.06**
Reg3d	Mm.33691	AB028625	1424009_at	21	10	0.48
Rhou	Mm.168257	AF378088	1449027_at	16	3	0.17
Rhou	Mm.168257	AF378088	1449028_at	27	6	0.26
Rnd1	Mm.274010	BE852181	1455197_at	19	36	**2.01**
Rnf135	Mm.22985	AK010429	1452289_a_at	76	160	**2.07**
Rnf43	Mm.440230	BC004781	1427008_at	62	32	0.49
Rnpepl1	Mm.200971	BB540667	1454753_at	96	32	0.32

Rpl5	Mm.399372	BM114165	1451077_at	18	8	0.45
Rps6kc1	Mm.220912	BM207149	1434563_at	26	10	0.38
Sat1	Mm.2734	NM_009121	1420502_at	64	11	0.17
Scarb2	Mm.297964	NM_007644	1460235_at	32	7	0.23
Sema3e	Mm.134093	NM_011348	1419717_at	24	10	0.45
Sfrs3	Mm.6787	NM_013663	1416151_at	17	10	0.48
Sh3bgrl	Mm.260760	BB248904	1436997_x_at	130	61	0.50
Sh3kbp1	Mm.286495	AK018032	1432269_a_at	96	41	0.44
Shcbp1	Mm.37801	NM_011369	1416299_at	1140	471	0.42
Slc16a12	Mm.74636	AV220703	1434188_at	34	17	0.45
Slc16a6	Mm.265874	NM_134038	1417884_at	20	91	**4.67**
Slc16a9	Mm.19325	AK004684	1429726_at	23	8	0.33
Slc35b2	Mm.289716	BC025875	1423927_at	116	29	0.24
Slc35b2	Mm.289716	AK003377	1429007_at	31	9	0.28
Slc4a10	Mm.314497	NM_033552	1417672_at	88	28	0.32
Slc4a3	Mm.5053	NM_009208	1418485_at	23	46	**2.10**
Slc6a13	Mm.258596	BC023117	1424338_at	10	27	**2.98**
Slco4c1	Mm.11662	AV024403	1437870_at	39	16	0.41
Slit2	Mm.289739	BG963150	1424659_at	10	29	**2.87**
Snx19	Mm.35084	BB283306	1436147_at	18	8	0.43
Socs1	Mm.130	AB000710	1450446_a_at	54	26	0.47
Sox2	Mm.65396	U31967	1416967_at	29	63	**2.22**
Sp5	Mm.423397	NM_022435	1422914_at	5	43	**8.12**
Spata13	Mm.149776	AV271736	1454656_at	69	32	0.43
Spry2	Mm.390759	BB529691	1436584_at	5	11	**2.15**
Stk10	Mm.8235	NM_009288	1417751_at	366	160	0.46
Stoml1	Mm.216502	AK007508	1452738_at	29	9	0.30
Suhw4	Mm.242791	BB430212	1457455_at	15	7	0.46
Sult1d1	Mm.6824	NM_016771	1448973_at	18	9	0.42
Sult2b1	Mm.271634	NM_017465	1417335_at	45	13	0.33
Synpo2l	Mm.35789	AK004253	1428295_at	1	5	**3.84**
Synpo2l	Mm.35789	BB322227	1447657_s_at	31	69	**2.26**
Syt12	Mm.262270	NM_134164	1422878_at	29	6	0.21
Syt7	Mm.182654	AV138438	1441927_at	165	39	0.21
Syt7	Mm.182654	AI854420	1460081_at	378	95	0.25
Tal1	Mm.439685	NM_011527	1449389_at	43	16	0.33
Tarsl2	Mm.35127	BQ176328	1434738_at	35	16	0.49
Tcfap2a	Mm.85544	BC021623	1426048_s_at	35	71	**2.15**
Tex15	Mm.280624	NM_031374	1420719_at	764	246	0.34
Tex261	Mm.391476	BF181445	1450965_at	222	78	0.34
Tex261	Mm.391476	AK013971	1452768_at	24	11	0.45
Thsd7b	Mm.380518	AV270900	1460627_at	15	7	0.43
Timp2	Mm.206505	M93954	1460287_at	20	11	0.45
Tirap	Mm.23987	NM_054096	1418685_at	71	35	0.47
Tirap	Mm.23987	BB365296	1457676_at	229	94	0.40
Tlr1	Mm.273024	AF316985	1449049_at	3	156	**58.02**
Tlr3	Mm.33874	NM_126166	1422782_s_at	75	151	**2.06**
Tmeff2	Mm.245154	NM_019790	1419073_at	24	57	**2.44**
Tmem14a	Mm.441478	AK017734	1428447_at	137	46	0.34
Tmem27	Mm.143766	AI314694	1435064_a_at	68	30	0.41
Tmem56	Mm.26088	BB667728	1434553_at	14	58	**4.08**
Tox	Mm.87051	BB547854	1425483_at	17	8	0.48
Tox	Mm.87051	BB547854	1425484_at	24	10	0.44
Tox	Mm.87051	BF020502	1442039_at	62	29	0.44
Tpm1	Mm.121878	AK002271	1423049_a_at	69	4	0.06
Tpm1	Mm.121878	M22479	1423721_at	61	14	0.24
Trim35	Mm.43871	BQ175280	1454650_at	494	212	0.44
Trpm6	Mm.215171	BM213868	1438877_at	243	124	0.49
Tslp	Mm.143716	NM_021367	1450004_at	14	4	0.37
Tspan1	Mm.45994	AV371704	1417957_a_at	112	51	0.49

Ttll9	Mm.44746	AK015740	1430865_s_at	12	5	0.35
Ttyh1	Mm.29729	NM_021324	1422694_at	19	52	**2.81**
Ttyh1	Mm.29729	BB560071	1426617_a_at	20	52	**2.57**
Ube2e3	Mm.1485	AW120830	1448671_at	7	23	**3.23**
Vangl2	Mm.36148	BB417279	1436118_at	12	5	0.50
Vps36	Mm.41453	AK013045	1452898_at	76	33	0.40
Vsnl1	Mm.27005	NM_012038	1420955_at	16	7	0.47
Wfdc15b	Mm.330764	NM_138685	1419195_at	29	15	0.49
Wipi1	Mm.35817	BC025560	1424917_a_at	28	10	0.37
Wipi1	Mm.35817	BB044002	1438709_at	26	14	0.47
Wipi1	Mm.35817	BI251603	1439060_s_at	136	52	0.38
Wipi1	Mm.35817	BG068076	1452392_a_at	55	18	0.33
Wipi1	Mm.35817	BI251603	1456624_at	22	9	0.40
Wnt7a	Mm.56964	AK004683	1423367_at	4	38	**7.67**
Wrnip1	Mm.286680	NM_030215	1448376_at	397	806	**2.02**
Xylb	Mm.219497	BB431728	1426706_s_at	81	18	0.23
Zbtb39	Mm.27258	AW489513	1443880_at	108	8	0.07
Zfp114	Mm.435485	BB794862	1457185_at	14	31	**2.08**
Zfp131	Mm.139115	BB833349	1459659_at	58	23	0.39
Zfp187		BB354728	1457285_at	24	74	**2.83**
Zfp282	Mm.440186	BB030565	1424297_at	64	21	0.33
Zfp282	Mm.440186	BB030565	1424298_at	22	6	0.25
Zfp398	Mm.169059	BB199476	1456639_at	27	13	0.44
Zfp41	Mm.87210	BB022304	1454927_at	136	288	**2.10**
Zfp42	Mm.285848	NM_009556	1418362_at	13	28	**2.07**
Zfp503	Mm.292401	BB447914	1423835_at	9	31	**3.05**
Zfp503	Mm.292401	BB447914	1423836_at	5	21	**3.42**
Zfp583	Mm.333558	AV174083	1439861_at	77	27	0.36
Zhx1	Mm.244931	NM_009572	1448875_at	87	27	0.31
Zik1	Mm.49441	BE824681	1433946_at	11	6	0.49
		BF227338	1431577_at	6	3	0.41
		AI195532	1435245_at	8	21	**2.85**
	Mm.387143	BE631223	1435872_at	141	64	0.47
	Mm.380256	AV365582	1437967_at	21	10	0.46
		BB138331	1439836_at	179	80	0.46
	Mm.151876	BB364961	1439887_at	59	28	0.47
	Mm.285452	AV380966	1440084_at	40	16	0.46
		BB667349	1441428_at	166	71	0.41
	Mm.384060	AI642706	1441818_at	25	8	0.34
	Mm.362032	AV111366	1443735_at	14	6	0.38
	Mm.376549	BB255018	1445275_at	16	8	0.47
		BB704012	1447173_at	15	6	0.39
	Mm.184776	BB545511	1447550_at	27	93	**3.32**
	Mm.370046	BB425316	1455722_at	90	41	0.44
	Mm.261326	BB457336	1457701_at	20	5	0.27
	Mm.361260	BG067824	1457850_at	335	152	0.46
		BB520860	1458145_at	76	37	0.46
		BB245422	1458212_at	15	7	0.46
		AW492552	1458463_at	12	6	0.49

*_a suffix, fully complementary to multiple alternative transcripts from the same gene; _s suffix, fully complementary to multiple transcripts from different genes; _x suffix, fully complementary to a unique transcript, but partial cross-hybridization with other sequences is expected; all other probesets are fully complementary to unique transcripts.
Some genes are represented by more than one probeset.
Bold indicates Tg/Ntg ratios that are greater than 1.

Table S10. Upregulated signal transduction genes	
Gene symbol	Gene name
AW742319	Butyrate-induced transcript 1
Axin1	Axin
Bmp7	Bone morphogenetic protein 7
Ccl2	Chemokine (C-C motif) ligand 2
Clic3	Chloride intracellular channel 3
Cxcr4	Chemokine (C-X-C motif) receptor 4
Depdc6	Expressed sequence R75183
Dgkz	Diacylglycerol kinase zeta
Dkk3	Dickkopf homolog 3 (Xenopus laevis)
Dvl1	Dishevelled, dsh homolog 1 (Drosophila)
Epha6	Eph receptor A6
Fcgr1	Fc receptor, IgG, high affinity I
Fgfr2	Fibroblast growth factor receptor 2
Fshr	Follicle stimulating hormone receptor
Gnat2	Guanine nucleotide binding protein, alpha transducing 2
Gnaz	Guanine nucleotide binding protein, alpha z subunit
Gpr146	cDNA sequence BC003323
Gpr20	G protein-coupled receptor 20
Gpr73l1	G protein-coupled receptor 73-like 1
Grm7	Glutamate receptor, metabotropic 7
Hck	Hemopoietic cell kinase
Htr5b	5-hydroxytryptamine (serotonin) receptor 5B
Il17r	Interleukin 17 receptor
Ilk	Integrin linked kinase
Itgae	Integrin, alpha E, epithelial-associated
Lgr6	Similar to VTS20631
Mapkbp1	Mitogen activated protein kinase binding protein 1
Myo9b	Myosin IXb
Oprd1	Opioid receptor, delta 1
Pace4	Paired basic amino acid cleaving system 4
Pdzrn3	semaF cytoplasmic domain associated protein 3
Ppm1l	Protein phosphatase 2a, catalytic subunit, epsilon isoform
Prkar2b	Protein kinase, cAMP dependent regulatory, type II beta
Rab24	RAB24, member RAS oncogene family
Rhof	Ras homolog gene family, member f (in filopodia)
Rnd1	RIKEN cDNA A830014L09 gene
Ror2	Receptor tyrosine kinase-like orphan receptor 2
Scrib	Scribble homolog 1 (Drosophila)
Slit2	Slit homolog 2 (Drosophila)
Socs3	Suppressor of cytokine signaling 3
Spry2	Sprouty homolog 2 (Drosophila)
Tnfrsf21	Tumor necrosis factor receptor superfamily, member 21
Traf5	Tnf receptor-associated factor 5
Wnt7a	Wingless-related MMTV integration site 7A

Table S2. EASE analysis of 1.4-fold downregulated transcripts		
Biological process*	List hits	EASE score
Sulfur metabolism	8	3.17E-03
Glutathione metabolism	4	1.79E-02
Sulfate assimilation	3	1.93E-02
Sulfur utilization	3	1.93E-02
Cell surface receptor linked signal transduction	34	3.15E-02
Cell adhesion	17	3.19E-02
*All over-represented categories are shown.		

Table S3. EASE analysis of 1.4-fold upregulated transcripts		
Biological process*	List hits	EASE score
Morphogenesis	38	9.82E-06
Development	51	2.15E-05
Organogenesis	30	1.89E-04
Inflammatory response	8	2.65E-04
Innate immune response	8	3.17E-04
Response to abiotic stimulus	12	1.57E-03
Response to chemical substance	8	2.06E-03
Behavior	8	2.31E-03
Response to external stimulus	18	2.41E-03
Pattern specification	8	2.59E-03
Learning	4	4.76E-03
Response to biotic stimulus	18	4.78E-03
Organismal physiological process	22	5.75E-03
Cell surface receptor linked signal transduction	26	5.76E-03
Response to wounding	8	6.41E-03
Regulation of biological process	62	6.66E-03
Immune response	13	6.83E-03
Embryonic morphogenesis	5	8.87E-03
Skeletal development	6	1.04E-02
Response to pest, pathogen, or parasite	9	1.12E-02
Response to external biotic stimulus	9	1.28E-02
Regulation of transcription	44	1.79E-02
Cell communication	52	1.82E-02
Regulation of nucleic acid metabolism	44	1.93E-02
Learning or memory	4	2.24E-02
Defense response	13	2.49E-02
Chemotaxis	5	2.51E-02
Taxis	5	2.51E-02
Signal transduction	44	2.65E-02
Regulation of physiological process	46	2.79E-02
G-protein coupled receptor signaling pathway	13	2.90E-02
Regulation of transcription, DNA-dependent	42	2.98E-02
Cell maturation	3	4.03E-02
Transcription	44	4.26E-02
Transcription, DNA-dependent	42	4.49E-02
Regulation of metabolism	44	4.88E-02
*All over-represented categories are shown.		

Table S4. Downregulated sulfur metabolism genes	
Gene symbol	Gene name
Chst11	Chondroitin 4-sulfotransferase
Gss	Glutathione synthetase
Gstk1	RIKEN cDNA 0610025I19 gene
Idh1	Isocitrate dehydrogenase 1 (NADP+), soluble
Mgst1	Microsomal glutathione S-transferase 1
Papss2	3′-Phosphoadenosine 5′-phosphosulfate synthase 2
Sult1d1	N-sulfotransferase
Sult2b1	Sulfotransferase family, cytosolic, 2B, member 1

Table S5. Downregulated cell surface receptor linked signal transduction genes	
Gene symbol	Gene name
2610028F08Rik	RIKEN cDNA 2610028F08 gene
6330442E02Rik	Hypothetical protein 6330442E02
Adora2b	Adenosine A2b receptor
Alk	Anaplastic lymphoma kinase
Atrnl1	Hypothetical protein LOC226255
AW551984	Expressed sequence AW551984
Bai1	Brain-specific angiogenesis inhibitor 1
Csnk2a2	Casein kinase II, alpha 2, polypeptide
Edg2	Endothelial differentiation, lysophosphatidic acid G-protein-coupled
Ednrb	Endothelin receptor type B
Epha3	Eph receptor A3
Epha7	Eph receptor A7
Gnai1	Guanine nucleotide binding protein, alpha inhibiting 1
Gnaq	Guanine nucleotide binding protein, alpha q polypeptide
Gpr125	RIKEN cDNA 3830613O22 gene
Gpr63	G protein-coupled receptor 63
Gpr84	G protein-coupled receptor 84
Gprk5	G protein-coupled receptor kinase 5
Homer1	Homer homolog 1 (Drosophila)
Hs1bp3	HS1 binding protein 3
Itgav	Integrin alpha V
Itgb2l	Integrin beta 2-like
Osmr	Oncostatin receptor
P2y5	Purinergic receptor (family A group 5)
Pcsk5	Proprotein convertase subtilisin/kexin type 5
Phip	Pleckstrin homology domain interacting protein
Ptprk	Protein tyrosine phosphatase, receptor type, K
Ptprs	Protein tyrosine phosphatase, receptor type, S
Pxn	Paxillin
Socs1	Suppressor of cytokine signaling 1
Stxbp4	Syntaxin binding protein 4
Tac2	Tachykinin 2
Tcf7l2	Transcription factor 7-like 2, T-cell specific, HMG-box
Tirap	Toll-interleukin 1 receptor (TIR) domain-containing adaptor protein

Table S6. Downregulated cell-adhesion genes	
Gene symbol	Gene name
Bysl	Bystin-like
C130076O07Rik	RIKEN cDNA C130076O07 gene
Cml2	Camello-like 2
Cntnap4	Contactin associated protein 4
Col13a1	Procollagen, type XIII, alpha 1
Col19a1	Procollagen, type XIX, alpha 1
Icam1	Intercellular adhesion molecule
Itgav	Integrin alpha V
Itgb2l	Integrin beta 2-like
Kitl	Kit ligand
Pard3	Par-3 (partitioning defective 3) homolog (C. elegans)
Pcdhb15	Protocadherin beta 15
Pcdhb17	Protocadherin beta 17
Prlr	Prolactin receptor
Ptprs	Protein tyrosine phosphatase, receptor type, S
Pxn	Paxillin
Scarb2	Scavenger receptor class B, member 2

Table S7. Upregulated morphogenesis genes	
Gene symbol	Gene name
Ank	Progressive ankylosis
Anxa2	Annexin A2
Arhgap15	Rho GTPase activating protein 15
Bmp7	Bone morphogenetic protein 7
Cobl	Cordon-bleu
Crb3	Hypothetical protein 5730439B18
Cxcl13	Chemokine (C-X-C motif) ligand 13
Cxcr4	Chemokine (C-X-C motif) receptor 4
Dpysl5	Dihydropyrimidinase-like 5
Egr2	Early growth response 2
Emx2	Empty spiracles homolog 2 (Drosophila)
Epb4.2	Erythrocyte protein band 4.2
Fgfr2	Fibroblast growth factor receptor 2
Gata4	GATA binding protein 4
Gli3	GLI-Kruppel family member GLI3
Hoxa1	Homeo box A1
Hoxd1	Homeo box D1
Hoxd13	Homeo box D13
Hoxd8	Homeo box D8
Ilk	Integrin linked kinase
Mbp	Myelin basic protein
Myl2	Myosin, light polypeptide 2, regulatory, cardiac, slow
Nedd9	Neural precursor cell expressed, developmentally down-regulated gene 9
Nos3	Nitric oxide synthase 3, endothelial cell
Nrp2	Neuropilin 2
Ostm1	Grey lethal osteopetrosis
Phlda2	Tumor-suppressing subchromosomal transferable fragment 3
Prelp	Proline arginine-rich end leucine-rich repeat
Prkar2b	Protein kinase, cAMP dependent regulatory, type II beta
Prkar2b	Protein kinase, cAMP dependent regulatory, type II beta
Rnd1	RIKEN cDNA A830014L09 gene
Ror2	Receptor tyrosine kinase-like orphan receptor 2
Runx2	Runt related transcription factor 2
Scrib	Scribble homolog 1 (Drosophila)
Slit2	Slit homolog 2 (Drosophila)
Socs3	Suppressor of cytokine signaling 3
Spry2	Sprouty homolog 2 (Drosophila)
Tpm3	Tropomyosin 3, gamma
Wnt7a	Wingless-related MMTV integration site 7A

Table S8. Upregulated development genes	
Gene symbol	Gene name
Ank	Progressive ankylosis
Anxa2	Annexin A2
Arhgap15	Rho GTPase activating protein 15
Axin1	Axin
Bmp7	Bone morphogenetic protein 7
Cd9	CD9 antigen
Cobl	Cordon-bleu
Crb3	Hypothetical protein 5730439B18
Cxcl13	Chemokine (C-X-C motif) ligand 13
Cxcr4	Chemokine (C-X-C motif) receptor 4
Dkk3	Dickkopf homolog 3 (Xenopus laevis)
Dpysl5	Dihydropyrimidinase-like 5
Dvl1	Dishevelled, dsh homolog 1 (Drosophila)
Egr2	Early growth response 2
Emx2	Empty spiracles homolog 2 (Drosophila)
Epb4.2	Erythrocyte protein band 4.2
Evx1	Even skipped homeotic gene 1 homolog
Fgfr2	Fibroblast growth factor receptor 2
Gata4	GATA binding protein 4
Gli3	GLI-Kruppel family member GLI3
Gsc	Goosecoid
Hoxa1	Homeo box A1
Hoxd1	Homeo box D1
Hoxd13	Homeo box D13
Hoxd8	Homeo box D8
Ilk	Integrin linked kinase
Mbd3	Methyl-CpG binding domain protein 3
Mbp	Myelin basic protein
Myl2	Myosin, light polypeptide 2, regulatory, cardiac, slow
Nedd9	Neural precursor cell expressed, developmentally down-regulated gene 9
Nos3	Nitric oxide synthase 3, endothelial cell
Nrp2	Neuropilin 2
Olfm1	Olfactomedin 1
Ostm1	Grey lethal osteopetrosis
Phlda2	Tumor-suppressing subchromosomal transferable fragment 3
Plxdc2	Tumor endothelial marker 7 related precursor
Prelp	Proline arginine-rich end leucine-rich repeat
Prkar2b	Protein kinase, cAMP dependent regulatory, type II beta
Rnd1	RIKEN cDNA A830014L09 gene
Ror2	Receptor tyrosine kinase-like orphan receptor 2
Runx2	Runt related transcription factor 2
Scrib	Scribble homolog 1 (Drosophila)
Six1	Sine oculis-related homeobox 1 homolog (Drosophila)
Slit2	Slit homolog 2 (Drosophila)
Socs3	Suppressor of cytokine signaling 3
Sox2	SRY-box containing gene 2
Spry2	Sprouty homolog 2 (Drosophila)
Tcf15	Transcription factor 15
Tpm3	Tropomyosin 3, gamma
Wnt7a	Wingless-related MMTV integration site 7A
Zfp41	Zinc finger protein 41

Table S9. Upregulated transcription genes	
Gene symbol	Gene name
Atbf1	AT motif binding factor 1
Bach2	BTB and CNC homology 2
Basp1	Brain abundant, membrane attached signal protein 1
Bcor	Bcl6 interacting corepressor
Carm1	Coactivator-associated arginine methyltransferase 1
Cebpd	CCAAT/enhancer binding protein (C/EBP), delta
Egr2	Early growth response 2
Emx2	Empty spiracles homolog 2 (Drosophila)
Evx1	Even skipped homeotic gene 1 homolog
Gata4	GATA binding protein 4
Gli3	GLI-Kruppel family member GLI3
Gls2	Liver mitochondrial glutaminase
Gsc	Goosecoid
Hes1	Hairy and enhancer of split 1 (Drosophila)
Hoxa1	Homeo box A1
Hoxd1	Homeo box D1
Hoxd13	Homeo box D13
Hoxd8	Homeo box D8
Irx1	Iroquois related homeobox 1 (Drosophila)
Junb	Jun-B oncogene
Lbx1h	Lady bird-like homeobox 1 homolog (Drosophila)
Mbd3	Methyl-CpG binding domain protein 3
Mxi1	Max interacting protein 1
Nfatc2	Nuclear factor of activated T-cells, cytoplasmic 2
Nfe2l3	Nuclear factor, erythroid derived 2, like 3
Nr2e3	Nuclear receptor subfamily 2, group E, member 3
Rbak	RB-associated KRAB repressor
Ripk4	Ankyrin repeat domain 3
Runx2	Runt related transcription factor 2
Six1	Sine oculis-related homeobox 1 homolog (Drosophila)
Sox13	SRY-box containing gene 13
Sox15	SRY-box containing gene 15
Sox2	SRY-box containing gene 2
Sp5	Trans-acting transcription factor 5
Tcf15	Transcription factor 15
Tcfap2a	Transcription factor AP-2, alpha
Tcfcp2l3	Grainyhead like 2 (Drosophila)
Trim30	Tripartite motif protein 30
Zfp235	Zinc finger protein 235
Zfp278	Zinc finger protein 278
Zfp41	Zinc finger protein 41
Zfp42	Zinc finger protein 42
Zfp62	Zinc finger protein 62
Znrd1	RIKEN cDNA 1110014N07 gene